A mechanistic model of small intestinal starch digestion and glucose uptake in the cow

RUNNING HEAD: SMALL INTESTINE STARCH MODEL FOR COWS

A mechanistic model of small intestinal starch digestion and glucose uptake in the cow

J. A. N. Mills,* J. France,*[1] J. L. Ellis,*† L. A. Crompton,‡ A. Bannink,§ M. D. Hanigan,# and J. Dijkstra,†

*Centre for Nutrition Modelling, Department of Animal and Poultry Science, University of Guelph, Guelph, ON N1G 2W1, Canada

†Animal Nutrition Group, Wageningen University, 6708 WD, Wageningen, the Netherlands

‡School of Agriculture, Policy and Development, University of Reading, Reading, RG6 6AR, UK

§Wageningen UR Livestock Research, 8219 PH, Lelystad, the Netherlands

#Department of Dairy Science, Virginia Tech, 2080 Litton Reaves, Blacksburg, VA, USA

[1]Corresponding author: jfrance@uoguelph.ca

ABSTRACT

The high contribution of postruminal starch digestion (up to 50%) to total tract starch digestion on energy-dense, starch-rich diets demands that limitations to small intestinal starch digestion be identified. A mechanistic model of the small intestine is described and evaluated with regard to its ability to simulate observations from abomasal carbohydrate infusions in the dairy cow. The seven state variables represent starch, oligosaccharide, glucose and pancreatic amylase in the intestinal lumen, oligosaccharide and glucose in the unstirred water layer (UWL) at the intestinal wall, and intracellular glucose of the enterocyte. Enzymatic hydrolysis of starch is modelled as a two stage process involving the activity of pancreatic amylase in the lumen and of oligosaccharidase at the brush border of the enterocyte confined within the UWL. Na^+ dependent glucose transport into the enterocyte is represented along with a facilitative GLUT2 transport system on the basolateral membrane. The small intestine is subdivided into three main sections representing the duodenum, jejunum and ileum for parameterisation. Further sub-sections are defined between which continual digesta flow is represented. The model predicted non-structural carbohydrate disappearance in the small intestine for cattle unadapted to duodenal infusion with R^2 = 0.92 and a root mean square prediction error (RMSPE) of 25.4%. Simulation of glucose disappearance for mature Holstein heifers adapted to various levels of duodenal glucose infusion yielded R^2 = 0.81 and a RMSPE of 38.6%. Analysis of model behaviour identified limitations to the efficiency of small intestinal starch digestion with high levels of duodenal starch flow. Limitations to individual processes, particularly starch digestion in the proximal section of the intestine, can create asynchrony between starch hydrolysis and glucose uptake capacity.

Key words: starch digestion, small intestine, glucose uptake, mechanistic model

INTRODUCTION

The need to satisfy the energy requirements of high genetic merit dairy cows during early lactation often results in the feeding of substantial quantities of starch rich concentrate. Coupled to this is the use of high starch corn silages as a main or primary forage component in many dairy production systems (Khan et al., 2015). The fate of dietary starch is highly variable and depends on many factors including starch type, processing and interaction with other diet components (Mills et al., 1999a,b; Moharrery et al., 2014; Patton et al., 2012) and maturity of corn at harvest (Hatew et al., 2016; Peyrat et al., 2016). This has significant implications for the productive capacity of the dairy cow (Nocek and Tamminga, 1991).

Previously, we developed a model for lactate metabolism in the rumen with a view to address the issue of rumen acidosis (Mills et al, 2014). Whilst starch may be highly degraded by rumen micro-organisms, up to 50% may escape undegraded to the small intestine, in particular with corn, sorghum and legumes (Mills et al., 1999a; Larsen et al., 2009), depending on the ration. The digestion of starch within the small intestine, followed by the absorption of the released glucose, may avoid the inefficiencies of rumen fermentation (Huntington et al., 2006; Reynolds et al., 2014). Digestion of up to 2.5 kg/d of starch in the small intestine of lactating dairy cows has been reported (Reynolds et al., 2014). However, starch reaching the small intestine is by nature less digestible than starch digested in the rumen. As starch flow to the small intestine increases, starch digestibility in the small intestine decreases, and there may be limits to the capacity of the small intestine for enzymatic hydrolysis of starch or glucose uptake by epithelial tissue (Mills et al., 1999b; Huntington et al., 2006; Reynolds et al., 2014). Subsequently, excessive fermentation in the hindgut of starch that escapes digestion in the small intestine may negatively affect fibre

digestion and may have negative effects on absorption of microbial lipopolysaccharides (Li et al., 2012). Published data regarding glucose flux across the small intestine in cattle shows highly variable results depending on diet fed or level of postruminal glucose infusion (Huntington and Reynolds, 1986; Reynolds et al., 1988; Reynolds et al., 1991). Patton et al. (2012) compared several models on accuracy of prediction of post-ruminal starch digestion. Even with the large intestine compensating for part of the variation in starch digestion in the small intestine, they still obtained substantial prediction errors of 15% and over 20% of observed means for corn-starch and non-corn starch, respectively. There is hence room for improvement of prediction of intestinal starch digestion. Complementary to improving empirical models (which include fractional rates of passage and digestion; e.g. Patton et al., 2012), is the study of factors which underlie such variation. The objective of the present study is to construct a mechanistic model that can be used to simulate the digestive metabolism of non-structural carbohydrate flowing through the small intestine of the dairy cow.

THE MODEL

The model is based on principles advanced by Mills et al. (1999b) and is illustrated in Figure 1. The level of aggregation adopted to describe the biological processes is similar to that used in previous modelling studies for the rumen and large intestine (Mills et al., 2014). Hence, the model can be considered alone as a tool for small intestinal starch digestion or as an element within a larger model of nutrient digestion and utilisation in the dairy cow. The model consists of three principal sections representing the duodenum, jejunum and ileum between which parameters describing enzyme activity, metabolite transport and intestinal physiology are varied according to literature values. These sections are further subdivided into subsections (2 in duodenum, 15 in

jejunum and 30 in ileum; see below for discussion) representing shorter lengths of intestine within which the state variables are represented. Division into subsections facilitates the simulation of digesta flow within each section (i.e., within duodenum, jejunum or ileum) as well as between sections. Equations representative of the model and abbreviations used to define model entities are listed in the Appendix. Associated parameters describing properties of the model and their values are given in Table 1. All pools are expressed in moles, with volume in litres (L) and time in hours (h). The flow equations are described by Michaelis–Menten or mass action forms. To describe non-structural carbohydrates in molar terms, molecular mass of non-polymerised and polymerised glucose is assumed to be 180 and 162 respectively. It is assumed that oligosaccharide resulting from starch hydrolysis contains an average of 5 glucose molecules.

Parameterisation

Intestinal Size and Digesta Passage. In the absence of other experimental observations, the length of the small intestine is set according to the observations of Gibb et al. (1992) for dairy cows at different stages of lactation. Whilst duodenal length is well characterised within the literature, the proportion of total length attributable to the jejunal and ileal sections is less clear, with little data available especially in the cow. Madge (1975) cites the ratio of duodenal, jejunal and ileal length as 1:4:7. However, most experimental observations for biological activity at these three points relate to measurements taken well within the bounds of the respective sections. Therefore, location-dependent parameters are set according to observed data for the mid duodenum, mid jejunum and terminal ileum (0.9 of ileal length). These parameters are extrapolated in a linear fashion between these three points. The proportions of small intestinal length accounted for by the duodenum, jejunum, and ileum are set at 0.02, 0.35 and 0.63

109 respectively. For the volume and surface area calculations, the small intestine is treated as a
110 cylinder of diameter 5 cm across all sections (Braun et al., 1995).

111 Duodenal nutrient inputs are determined by the composition of infusate or of duodenal
112 nutrient flow reported in the investigations being used for model simulations. Passage of digesta
113 between the intestinal sections and subsections is represented as a fractional rate (k_p) assuming
114 mixing within each section due to myoepithelial contractions (Ruckebusch, 1988). Fractional
115 passage rate between the luminal pools is a function of total mean retention time (**MRT**) for the
116 small intestine. The total MRT in the small intestine is dependent on k_p and intestinal length.
117 Where experimental observations are lacking, k_p is set according to Cant et al. (1999) who
118 observed a rate of 16 m/h in a mature dairy heifer (507 kg). Whilst in reality passage along the
119 small intestine is pulsatile (Ruckebusch, 1988), for simplicity the model assumes a continuous
120 digesta flow between the luminal pools of the intestinal subsections.

121 Small intestinal digesta volume is set at 13% of theoretical lumen volume (12.5 L for a
122 dairy cow with small intestinal length assumed to be 48 m) (Gibb et al., 1992). Water absorption is
123 assigned a fractional rate of 2% of volume per h. This is calculated assuming typical abomasal
124 outflows of 3% dry matter (DM) and ileal outflows of 8% (DM) for a MRT of 2.5 h and hence it is
125 the net result of water absorption from and water influx (with secretions) into the intestinal lumen.
126
127 ***The Intestinal Lumen***

128 *Luminal Starch (Sl).* Inputs to the luminal starch pool are direct outputs from the
129 equivalent pool in the previous section. The input to the first duodenal section is the output from
130 the rumen, assuming no changes in starch flow occur in omasum and abomasum. The outputs
131 from the luminal starch pool are passage or hydrolysis to luminal oligosaccharide. The potential

hydrolysis of the starch is represented by starch digestion turnover time, which is discussed in more detail below under the heading 'Luminal α-Amylase'. Other factors influencing the rate of hydrolysis are the concentration and activity of pancreatic amylase, both of which are described below.

Luminal Oligosaccharide (Ol). Inputs to the oligosaccharide pool are directly from abomasal infusions (in the duodenum) or from outflows of the previous section. Outflows are via passage along the intestine or diffusion into the unstirred water layer (UWL). The diffusion coefficient for oligosaccharide ($k^{(d)}_{Ol,OlOu}$) is set at 0.0089 cm^2/h by adjusting the glucose diffusion coefficient for the difference in molecular radius (assumed to be proportional to the cube root of molecular weight) of oligosaccharide and glucose.

Luminal Glucose (Gl). For typical dietary situations it is assumed that glucose flow from the rumen (via the abomasum) is negligible. Thus in the present model, glucose may only enter the intestinal lumen via infusion at the abomasum. Outputs from the luminal pools are via passage along the intestine or diffusion into the UWL. The diffusion rate constant is discussed in the UWL section.

Luminal Digesta pH. The pH of the luminal contents can vary considerably between the duodenal and ileal sections of the small intestine. The acidic chyme entering the duodenum (pH 2.5) is buffered by pancreatic secretions rich in bicarbonate (pH 8) (Walker et al., 1994 Pierzynowski et al., 1988). Armstrong and Beever (1969) reviewed the observations of pH distribution throughout the ruminant small intestine in relation to the pH optima of various carbohydrases and concluded that maximal starch hydrolysis would occur in the proximal jejunum. Whilst most literature data confirm the general increase in luminal pH as digesta moves from the duodenum to the ileum, the actual acidity and rate of change along the tract seems to vary

considerably depending on the particular investigation and diet fed. Russell et al. (1981) fed steers either a lucerne only diet or lucerne diets with increasing corn. Duodenal pH (at 10% of intestinal length) was similar for all diets (pH 6.0 – 6.2) although the pH increase towards the ileum was greatest for the diets with least concentrate (ileal pH 7.2). Earlier studies report much lower pH values towards the duodenum. MacRae (1967) observed a pH range at the duodenum of 2.6 – 3.5, with an ileal pH between 8.0 and 8.3. Lennox and Garton (1968) monitored luminal pH in sheep fed grass cubes and observed pH ranges at the proximal jejunum, upper jejunum and distal jejunum of 2.5 – 4.0, 3.9 – 5.0 and 7.2 – 7.9 respectively. Unpublished data from Holstein dairy cows (Reynolds, 2000) indicates a pH of approximately 2.3 at the proximal duodenum and 8.3 at the terminal ileum. Low duodenal pH measurements are obtained where the sampling site is proximal to the pancreatic ducts, as with the results of Russell et al. (1981) and reported by Owens et al. (1986), confirming a substantial rise in luminal pH following pancreatic secretion (> pH 6.0). In the model, duodenal luminal pH is set according to observed values and rises in a linear manner to pH at the terminal ileum. Where experimental observations are not available these values are set at 6.0 and 8.0, respectively.

Luminal α-Amylase (Al). The first stage of starch digestion in the model is hydrolysis in the intestinal lumen via the action of pancreatic amylase. The product of this reaction is oligosaccharide (see below), and amylase activity is dependent on the quantity secreted and the pH of the intestinal lumen. There is only limited data concerning pancreatic amylase secretion in dairy cows, although various theories as to control mechanisms have been postulated (Fushiki and Iwai, 1989; Croom et al., 1992). Detailed representation of neural and hormonal regulatory mechanisms is beyond the scope of the present model. However, nutritional influences particularly concerning interactions with feed carbohydrate are considered. Due to the moderating effect of the rumen on

178 digesta flow, in contrast to non-ruminants, the flow of ruminant pancreatic secretion is relatively
179 constant irrespective of feeding behaviour (Pierzynowski, 1986; Walker and Harmon, 1995).
180 Pancreatic fluid secretion rate in young calves is in the range 0.33 – 0.49 mL/kg body weight
181 (**BW**)·h $^{-1}$ (Pierzynowski, 1989; Khorasani et al., 1990). The majority of observations indicate a
182 similar range for mature cattle (0.26 – 0.57 mL/kg BW·h $^{-1}$), although the influence of diet is
183 pronounced. Pierzynowski et al. (1988) recorded an increase in pancreatic secretion from 0.57 to
184 0.91 mL/kg BW·h $^{-1}$ when dry cows were fed isoenergetic and isonitrogenous rations with
185 molasses rather than grain as the energy source. Under typical nutritional management there is
186 approximately 12 mg total protein in bovine pancreatic fluid (Walker et al., 1994; Walker and
187 Harmon, 1995) of which less than 2% is amylase (Keller et al., 1958). Harmon (1993) reviewed
188 the literature and concluded that increased postruminal carbohydrate in the form of starch or
189 glucose decreases pancreatic amylase secretion whilst increasing energy intake raises secretion.

190 The model representation allows for increased pancreatic secretions for cows on a high
191 plane of nutrition whilst facilitating a decrease in the concentration of amylase in pancreatic
192 secretion with increased starch or glucose presence. Whilst Russell et al. (1981) observed a
193 doubling in pancreatic amylase activity for homogenised pancreatic tissue in steers fed at either
194 twice or three times maintenance relative to those at maintenance, they did not record fluid
195 secretion rates. In the model, the increase above the basal level of fluid secretion ($v^{**}_{Al,PfAl}$) is
196 sigmoidal and set to yield a doubling in total secretion between 1 and 2 times maintenance feeding
197 (Equation 1.5). The maximum rate of secretion ($v^{*}_{Al,PfAl}$) is arbitrarily set at 0.8 mL/kg BW·h $^{-1}$
198 based on the observations described above. The response to duodenal starch delivery (Equation
199 1.6) is inverse to that for energy intake. Minimum concentration of amylase in pancreatic fluid

($v^{**}_{Al,PpAl}$) is set at 10.0 U/mg fluid protein, based on observations by Walker and Harmon (1995). One unit (U) equates to 60 μmol of oligosaccharide released per h (hence $v_{Sl,SlOl}$ = 60 μmol/h). The maximum concentration of amylase ($v^*_{Al,PpAl}$) and the rate of duodenal starch or glucose delivery at which amylase concentration is half maximal ($M_{Al,PfAl}$) are set according to the data of Walker and Harmon (1995) at 22 U/mg fluid protein and 0.21 mol/h, respectively. The affinity of amylase for starch ($M_{Sl,SlOl}$) is set at 21.6 mmol/L (Russell et al., 1981) with a modification for starch hydrolysis based on a reference digestion turnover time (T^*_{Sl}) of 11.8 h for corn starch (Cone, 1991). Starch hydrolysis by pancreatic amylase depends on starch source and is set according to the observations of Cone (1991) who used pancreatin in vitro to degrade a range of starches over 4 h incubations. The digestion turnover time of starch (T_{Sl}) is calculated as the reciprocal of the fractional hydrolysis rate constant.

The optimum pH for pancreatic amylase activity ($v^{(o)}_{pH,SlOl}$) in cattle is 6.9 and activity declines substantially above and below this optimum (Russell et al., 1981). The response of amylase activity to pH is described by a Gaussian type equation (Equation 2.5), with the steepness parameter ($\theta_{Sl,SlOl}$ = 0.6, SE ± 0.15, R^2 = 0.68) fitted to describe the data of Russell et al. (1981) and Rosenblum et al. (1988).

The Unstirred Water Layer

To facilitate estimates of metabolite concentrations and diffusion parameters, the thickness of the UWL is set at 40 μm based on observations for human jejunal tissue (Levitt et al., 1992). In line with the observations of Lucas (1983), pH of the UWL is independent of luminal pH, with values of 6.1, 6.1, and 7.1 for duodenal, mid-jejunal and terminal ileal sections, respectively.

UWL Oligosaccharide (Ou). Input into the UWL oligosaccharide pool is from diffusion across the UWL, whilst outputs are diffusion into the lumen or hydrolysis to glucose via the action of brush border oligosaccharidase. Parameters for enzymatic hydrolysis are discussed below under the heading 'UWL Oligosaccharidase', and assumptions for diffusion rates were set out in the previous section 'The Intestinal Lumen'.

UWL Glucose (Gu). Inputs to the UWL glucose pool are from hydrolysis of UWL oligosaccharides, and from diffusion across the UWL (from lumen and from blood). Outputs are diffusion into the lumen and the blood and uptake into the epithelial cells by SGLT1. Pappenheimer and Reiss (1987) promote the concept of solvent drag induced paracellular transport as a significant contributor to glucose absorption in the small intestine of rats. Pappenheimer and Reiss (1987) indicate that where luminal glucose concentrations are greater than 250 mM, paracellular movement of glucose exceeds that for the transcellular route. However, Ferraris et al. (1990) suggest a physiological range in luminal glucose concentration for non-ruminants of 5 – 50 mM, whilst ruminants tend to show even lower concentrations (Bauer, 1996). Therefore, paracellular glucose flux is likely of limited significance in normal feeding situations. This is confirmed by the observations of Krehbiel et al. (1996) who infused 2-deoxyglucose (not transported by sodium dependent glucose co-transporter SGLT1; further explanation follows) into the duodenum of steers and recovered only 7% in the portal vein. However, the absolute significance of paracellular glucose transport is still unknown, especially as glucose may enter the lymphatic drainage and not the portal circulation (Largis and Jacobs, 1971). The influence of localised high glucose concentrations at the UWL may also be significant (Pappenheimer and Reiss, 1987). Meddings and Westergaard (1989) demonstrated that the uptake of luminal glucose in the rat is best described by a carrier system and a diffusion component across the UWL.

Therefore, a simple paracellular diffusion component is represented in the model between glucose at the UWL and glucose in the blood, assuming a diffusive surface area based on that for epithelial cell junctions of 4% of total brush border surface area (Krstic, 1979). The diffusion coefficient ($k^{(d)}_{Gu,GuGb}$) is set at 2.412×10^{-2} cm^2/h (Levitt et al., 1992).

UWL Oligosaccharidase. Oligosaccharidase activity is associated entirely with the brush border of the enterocyte (Harmon, 1993) and therefore the hydrolysis of oligosaccharide to glucose only occurs within the UWL. The ability of ruminants to regulate oligosaccharidase activity per unit of intestine appears limited. Reports of adaptive regulation in response to carbohydrate intake (Janes et al., 1985) are likely to be the result of changes in intestinal length as energy intake increases (Harmon, 1993). Therefore, the mean maximum activity is held constant and set according to the data of Kreikemeier et al. (1990) at 0.25, 1.0 and 0.72 U/cm^2 brush border membrane for the mid-duodenum, mid-jejunum and terminal ileum, respectively. One unit of activity represents 60 μmol glucose produced per hour and therefore $v^*_{Ou,OuGu}$ = 60 μmol/h. A similar distribution was reported by Coombe and Siddons (1973). The model employs a Gaussian type equation (Equation 6.7) fitted to the data of Coombe and Siddons (1973) to describe the activity of oligosaccharidase as affected by the UWL pH with a pH optimum of 6.0 and a steepness parameter ($\theta_{Ou,OuGu}$) of 0.19 (SE ±0.0068, R^2 = 0.98). The affinity for oligosaccharide is set at 4.3 mmol/L, assuming 70% maltase activity (affinity K_m = 2.3 mmol/L, mean of Siddons (1968) and Eggermont (1969)) and 30% isomaltase activity (K_m = 9.1 mmol/L, Coombe and Siddons (1973)).

Enterocyte Metabolism

In the absence of ruminant data, the cytoplasmic depth of the columnar epithelial cells is set at 25 μm according to observations from rabbits (Stevens, 1992), allowing calculation of enterocyte volume.

Na^+ Dependent Uptake of Glucose by SGLT1. The majority of glucose transport into the epithelial cells occurs via a sodium (Na^+) dependent glucose transporter (SGLT1) (Shirazi-Beechey et al., 1995; Dyer et al., 2003) present on the brush border membrane. Hence, transport of glucose into the epithelial cell obeys saturation kinetics, limited by the affinity of SGLT1 for glucose, the maximum uptake rate of glucose per unit of SGLT1 and the quantity of transporter protein present at the membrane. The kinetic properties of SGLT1 have been determined in vitro using brush border membrane vesicles that remove the influence of the unstirred water layer, otherwise present in vivo. Therefore, whilst in vivo estimates of the affinity of SGLT1 for glucose range from 6 to 23 mmol/L (Ferraris et al., 1990), in vitro results using vesicles show the true K_m be between 0.06 and 0.15 mmol/L (Bauer et al., 1997; Zhao et al., 1998). Therefore, $M_{Gu,GuGe}$ is set at 0.1 mmol/L. Maximum glucose uptake rates by SGLT1 per unit of intestinal epithelia vary depending on the luminal glucose presence or degree of adaptation to a particular diet (Hediger and Rhoads, 1994; Bauer, 1996). Diamond and Karasov (1987) demonstrated a 1.5% increase in glucose transporter activity for every 10% increase in dietary sugar level for mice fed isoenergetic diets. Assuming that the signal mechanism for regulation is in the proximal duodenum, $v_{Gu,GuGe}$ is dependent on non-structural carbohydrate entry to the small intestine (Equation 5.9). Since the model's purpose is to simulate the adapted state, and not transition between diets, up-regulation is assumed to have occurred. Bauer et al. (1995) observed a basal transport capacity of 960 mmol glucose/d in steers fed lucerne hay with or without carbohydrate infusion. Therefore, assuming a

small intestinal length of 35 m, the mean transport capacity for these steers was 0.73 μmol/cm^2/h intestinal epithelium, a value that has been adopted within the model ($v^{**}_{Gu,GuGe}$). Relatively high basal transporter density allows more efficient utilisation of transient nutrient inputs. Despite evidence suggesting regulation of the maximum SGLT1 capacity to meet or exceed luminal glucose supply in a variety of herbivores (Ferraris et al., 1990), this degree of adaptation in cattle has been questioned (Cant et al., 1999; Lohrenz et al., 2011). It is logical to assume an upper limit to active transport capacity irrespective of luminal glucose delivery. Invariably, the highest transport rates are observed at the pre-ruminant stage of development on milk based diets. Therefore, an absolute mean maximum uptake rate of glucose by SGLT1 ($v^{*}_{Gu,GuGe}$) is set at 29.2 μmol/cm^2/h brush border membrane according to data for lambs maintained on a milk-based diet for 5 weeks where transport capacity was 40 times basal levels (Shirazi-Beechey et al., 1991). Based on observations with brush border vesicles from a mid-lactation Holstein cow (Zhao et al., 1998), SGLT1 transport capacity ($v^{*}_{Gu,GuGe}$, $v^{**}_{Gu,GuGe}$) is distributed at a ratio of 0.66:1.0:0.12, between the mid-duodenum, mid-jejunum and terminal ileum, respectively.

Glucose in the Enterocyte (Ge). The inputs to the intracellular glucose pool are from luminal uptake by SGLT1 (Equation 7.2) and from blood by Na+ independent facilitated diffusion involving GLUT2 transport proteins at the basolateral membrane (Equation 7.3). There are two outputs, one via GLUT2 to the blood (Equation 7.4) and the other via oxidation in the enterocyte (Equation 7.5). Carbohydrate infusion studies frequently report a significant disparity in portal glucose appearance relative to disappearance in the intestine (Kreikemeier and Harmon, 1995). This is due to glucose oxidation by the visceral tissues in order to satisfy the energetic requirements of protein turnover and ion transport. Glucose utilisation by the small intestinal

311 mucosal tissue is estimated to enable a prediction of net glucose flux to the blood. Energetic
312 requirements of the mucosal tissue are calculated assuming that there is a basic energy
313 requirement for protein turnover (0.02 mmol ATP/g mucosa/h) and ion transport (0.031 mmol
314 ATP/g mucosa/h) in the fasted state (Gill et al., 1989). This equates to a combined glucose
315 requirement for protein turnover and ion transport of 0.0043 mmol glucose/g mucosa/h. According
316 to the observations of Kreikemeier et al. (1990), there is 0.15 g mucosa/cm^2 intestinal epithelium.
317 Added to these requirements are the energy costs associated with Na^+ dependent transport of
318 amino acids and glucose from the intestinal lumen to the epithelial cytosol. Amino acid uptake is
319 an input into the model based on experimental observations, with a requirement of 0.66 mmol
320 ATP/mmol amino acid as calculated by Gill et al. (1989). For glucose transport, a stoichiometry of
321 3 mol of glucose transported per mole of ATP hydrolysed yields a requirement of 0.33 mmol
322 ATP/mmol glucose (Gill et al., 1989). Therefore, the corresponding glucose requirements in the
323 model for oxidation during glucose transport ($R_{Ge,GuGe}$) and amino acid transport ($R_{Gu,AuAe}$) are
324 0.028 and 0.055 mmol glucose per mmol glucose and amino acid respectively.

325 In non-ruminants, energy requirements for enterocyte metabolism are met primarily by
326 glutamine oxidation (25 – 40% of total CO_2 production), with glucose oxidation only accounting
327 for 6 – 10% of CO_2 production (Windmueller and Spaethe, 1974; Hanson and Parsons, 1977;
328 Windmueller, 1982). However, Okine et al. (1995) observed that between 69 and 76% of energetic
329 requirements are met by glucose for bovine enterocytes in vitro with the remainder met by
330 glutamine oxidation. Therefore, the calculated energy requirements of the mucosa (mol ATP/h)
331 are met assuming a non-limiting supply of glutamine, with glucose oxidation supplying a
332 maximum of 70% of the total requirement for ATP and glucose is the preferred substrate. The fate
333 of metabolised glucose is set at 18% through complete oxidation to CO_2, 36% through lactate,

334 38% through glutamate and 8% through alanine (Okine et al., 1995). For calculation of ATP yield,
335 lactate and alanine are assumed to be lost to the circulation. Yield of ATP from complete
336 oxidation to CO_2 is 36 mol/mol glucose and from glutamate it is 14 mol/mol glutamate (Stryer,
337 1995). Therefore, the mean ATP yield per mol glucose metabolised by the epithelium is set at 11.9
338 mol.

339 *Facilitated Diffusion from the Enterocyte*. There is GLUT2 glucose transport from the
340 epithelial tissue to the blood (Thorens, 1993; Breves and Wolffram, 2006). Zhao et al. (1998)
341 showed that the distribution of GLUT2 in late lactation Holstein cows was similar to that reported
342 for humans (Burant et al., 1991). Northern blot analysis of GLUT2 mRNA demonstrated
343 considerably greater presence in the liver than in the kidney or duodenum (Zhao et al., 1998).
344 However, details of the nutritional management for the cows were not given and data regarding
345 the ability of the epithelial tissue to upregulate GLUT2 transporter presence in the bovine appears
346 to remain unavailable. Thorens (1993) reviewed the studies concerning GLUT2 adaptation to
347 intestinal glucose delivery and concluded that the rate of glucose transport through the basolateral
348 membrane after an acute exposure to increased glucose may result from changes in the intrinsic
349 activity of the transporter, whereas chronic exposure may increase GLUT2 presence. Cheeseman
350 and Harley (1991) showed that from a range of carbohydrate components only glucose and
351 fructose influenced GLUT2 presence in rat small intestine. Kellett and Helliwell (2000) stated that
352 GLUT2 quantity in rat jejunum doubled when luminal glucose concentration was increased from 0
353 to 100 mmol/L. Whilst Kellett and Helliwell (2000) reported a single saturation constant to
354 describe the affinity of GLUT2 for glucose (K_m = 56 mmol/L), the kinetics of glucose efflux from
355 the epithelial cell to the blood and uptake from the blood to the cell are in fact asymmetrical.
356 Maenz and Cheeseman (1987), using basolateral membrane vesicles (BLV) from rat jejunum,

showed the mean maximum velocity (V_{max}) for glucose efflux to be 0.20 ± 0.01 nmol glucose/mg BLV protein/sec with a K_m of 23 ± 2 mmol/L glucose, whilst glucose uptake gave a V_{max} of 1.14 ± 0.14 nmol glucose/mg BLV/sec and a K_m of 48 ± 5 mmol/L glucose. Such asymmetrical kinetics allows for an efficient glucose delivery system to the blood whilst minimising the reverse flux of glucose from the blood to the epithelial tissue. Hence, $M_{Ge,GeGb}$ and $M_{Gb,GbGe}$ are set at 23 and 48 mmol/L, respectively. In the absence of data specific to the dairy cow, basal maximum uptake rate from the cytosol by GLUT2 ($v^{**}_{Ge,GeGb}$) is set at 12.2 µmol/cm^2/h as measured in isolated rat enterocytes by Cheeseman and Harley (1991) and in line with Lohrenz et al. (2011), the distribution of GLUT2 is equal for each intestinal section. Calculation of basal maximal transport activity assumes 0.15 g mucosa/cm^2 basolateral membrane (Kreikemeier et al., 1990). The recruitment of additional GLUT2 and hence an increase in $v_{Ge,GeGb}$ is related to an increase in luminal NSC flow (Equation 7.4) with $v^{*}_{Ge,GeGb}$ set at 4 times basal level (Cheeseman and Maenz, 1989) and $M_{NSC,GeGb}$ set at 75 mmol/L duodenal NSC flow/h, as for the up-regulation of SGLT1.

The Blood

Blood Glucose (Gb). Plasma glucose concentration represents that of the mesenteric plasma pool in contact with the basolateral membrane of the intestinal epithelium. The concentration of blood glucose is held constant, since a full interpretation of portal drained viscera (**PDV**) metabolism is beyond the scope of the model. Where observations of blood glucose concentration are not available, estimates of 4 mmol/L can be used for cows (Reynolds and Huntington, 1988; Reynolds et al., 1991). The kinetics of glucose flux to and from the epithelial

tissue are described in the GLUT2 section whilst the calculation of net glucose flux is explained under Enterocyte Metabolism.

Model Summary

The differential equations for the 7 state variables in each of the 47 sub-sections of the small intestine, representing the nutrient pools in the lumen, the UWL and epithelial tissue, are integrated numerically for a given set of initial conditions and parameter values. The model was written in the Advanced Continuous Simulation Language (**ACSL**) (Mitchell and Gauthier Associates, 1995). A fourth-order fixed-step-length Runge-Kutta method with an integration interval of 0.25 min was used. The results presented were obtained by running the model until a steady state was achieved.

Model Evaluation

The model was initially evaluated against its ability to simulate the duodenal glucose infusion study of Cant et al. (1999) involving mature Holstein heifers adapted to the level of glucose supply. Infusion studies utilising adapted animals are rare, the other principal study being that of Bauer et al. (1995). However, Bauer et al. (1995) do not report small intestinal starch or glucose disappearance. To challenge the model further, a data set for small intestinal NSC disappearance was gathered from infusion studies utilising unadapted cattle. These were: the starch, dextrin, and glucose infusions (each at 20, 40 and 60 g/h) of Kreikemeier et al. (1991), the 10 and 20 g/h duodenal glucose infusions of Krehbiel et al. (1996), the glucose, starch and dextrin infusions (each at 66 g/h) of Kreikemeier and Harmon (1995), and the duodenal corn starch and ruminal casein infusion of Taniguchi et al. (1995).

401 Walker and Harmon, (1995) showed that 53% of starch hydrolysate (or dextrin) consisted
402 of glucose chain lengths of 7 or less. To accommodate this product within the model scheme, 30%
403 of starch hydrolysate is assumed to enter the luminal oligosaccharide pool directly (approx. 5
404 glucose molecules or less), with the remainder entering the duodenal starch pool.

405 Regression analysis between observed and predicted values was used to demonstrate
406 model performance. Error of prediction is estimated from the calculation of root Mean Square
407 Prediction Error (**rMSPE**) and expressed as a percentage of the observed mean, where:

408 $$\text{MSPE} = \sum (O_i - P_i)^2 / n$$

409 where $i = 1, 2, \ldots, n$; n is the number of experimental observations and O_i and P_i are the observed
410 and predicted values (Bibby and Toutenburg, 1977). The MSPE is decomposed into overall bias of
411 prediction, deviation of regression slope from one and the disturbance proportion (Bibby and
412 Toutenburg, 1977).

413 The response of the model to changes in parameter values (± 50%, except ± 20% for pH)
414 was tested in order to demonstrate sensitivity. The sensitivity and behavioural analyses were
415 performed for a 650 kg dairy cow consuming 22 kg dry matter (DM) at 11 MJ metabolisable
416 energy (ME) per kg DM, with an inflow or infusion of 2.0 kg wheat starch and 2.5 kg of ground
417 corn starch per day. This level of infusion is comparable with the highest observed duodenal
418 starch flows in the literature (McCarthy et al., 1989), with the aim of investigating the rate limiting
419 steps to the digestive and absorptive processes. Results of the sensitivity and behavioural analyses,
420 together with other aspects of model evaluation, are presented in the next section.
421

RESULTS

Comparison between Observations and Predictions

Figure 2 shows the comparison between model predictions and observations of ileal glucose flow in 4 adapted dairy heifers with increasing levels of duodenal glucose infusion (250 – 700 mmol/h) (Cant et al., 1999). There is good agreement between the observed and predicted values (R^2 = 0.81) although the small sample gives a high root MSPE (RMSPE) of 38.6%. Figure 2a shows a move away from the line of unity as glucose infusions increase. Figure 2b demonstrates how observed ileal glucose flow reached a plateau beyond 580 mmol/h infusion, whereas the model was unable to simulate this occurrence. It is difficult to ascertain the precise reason for this observed reduction in ileal glucose flow per unit of glucose infusion, although it may relate to the pattern of SGLT1 up-regulation in vivo and the comparatively short periods of adaptation to glucose infusions (3 d). Another explanation could be that the model underestimated the contribution of paracellular diffusion from the digesta to the blood, particularly at high concentrations of luminal glucose. However, the general agreement between observed and predicted results for the lower range of glucose concentrations, more likely to be encountered under normal nutritional management is encouraging.

Figure 3 displays a regression between observed and predicted small intestinal NSC disappearance for cattle unadapted to NSC infusions. The high R^2 (0.92) shows good agreement between the data and a lower RMSPE (25.4%) than for the simulation of glucose infusion in Figure 2a. The trend for under-prediction of luminal NSC removal at higher levels of observed disappearance is surprising and in contrast to results in Figure 2a. The unadapted animals should have a lower capacity to transport glucose and a reduced carbohydrase activity. It is possible that

445 certain internal parameters are more influential than any effect of dietary adaptation (see
446 sensitivity analysis).

447 Figure 4 displays a correlation between the observed net PDV flux of glucose in the same
448 cattle as for Figure 3, and the simulated net release of glucose from the enterocytes to the blood.
449 As expected, the *y*-intercept indicates a basal level of glucose release to the blood from the small
450 intestine (34 mmol/h), below which no net PDV flux is observed. However, the rate of increase in
451 simulated net glucose flux to the blood is too slow to support the observed increase in PDV
452 glucose flux. This is a clear indication of an overestimate of metabolism of luminal glucose by the
453 model; arterial glucose is a major source of glucose used by enterocytes. This may also be caused
454 by an overestimate of the total contribution of glucose to enterocyte metabolism, especially in the
455 presence of competing substrates such as glutamine. The in vitro measurements for dairy cattle
456 enterocytes that were used for model parameterisation (Okine et al., 1995) may not be
457 immediately applicable in vivo. Indeed, the results of Okine et al. (1995) are somewhat
458 contradictory to the more extensive data for other species, especially non-ruminants (Windmueller
459 and Spaethe, 1974; Windmueller, 1982). Over-estimates of intestinal length will also unduly
460 increase enterocyte glucose demand. Finally, microbial fermentation of glucose within the small
461 intestine was not included in the model, and this may lead to a difference between small intestinal
462 disappearance of starch and portal appearance of glucose. Gilbert et al. (2015) observed more than
463 50% of small intestinal starch disappearance to be due to fermentation in milk-fed calves fed
464 starch in milk replacer twice daily. At present, it is unclear if fermentation of starch has such a
465 significant role in mature cows fed solid feed leading to a much more gradual flow of starch to
466 into the small intestine.
467

Sensitivity and Behavioural Analyses

Small Intestinal Starch Flow. As starch spends more time in the small intestine it is subject to increasing opportunity for enzymatic hydrolysis. Therefore, digestibility increases and Figure 5a confirms this type of behaviour in the model. Beyond 4.5 h MRT, the digestion of starch is almost complete. The rate of decline in digestibility below 4.0 h MRT is high (20%/h). This supports the findings summarised from the literature by Reynolds et al. (2014), Mills et al. (1999b) and Nocek and Tamminga (1991) who report a declining small intestinal starch digestibility with increasing postruminal starch flow. Figure 5a indicates that the significance of pancreatic amylase activity as a limit to starch digestion increases as MRT declines. Figure 5b demonstrates the corresponding decline in glucose delivery to the blood. The rate of decline in net blood glucose flux increases as MRT declines because the proportion of flux attributed to glucose oxidation for maintenance of the enterocyte increases. It should be noted that Figure 5b applies primarily to constant starch infusions with increasing MRT. Where digesta flow rate increases in association with starch flow, there is a compensatory elevation in total starch availability for hydrolysis.

Luminal pH. Figures 6a, b, c highlight the benefits of maintaining duodenal digesta pH between 6 and 6.5. These simulations were run assuming a constant ileal digesta pH due to the extensive buffering capacity in this region of the intestine (Owens et al., 1986).Although the optimal pH for amylase is 6.9, a slightly reduced duodenal pH (6.5) with a gradual rise toward optimum levels at the jejunum resulted in a beneficial effect). Figures 6c, d are evidence of the need for synchronisation between the hydrolysis and uptake processes. Low duodenal pH limits starch hydrolysis initially, and this delay shifts the availability of glucose in the UWL further towards the ileum where SGLT1 capacity is most limiting. Hence, where small intestinal starch

flow is high, digesta pH seems to have as much an effect on glucose uptake as it does directly on starch hydrolysis.

Intestinal Size. The description of small intestinal physiology can substantially affect net glucose flux. It is self-evident that as the proportion of ileum increases relative to the proximal regions of the intestine, the total capacity to transport glucose declines (Figure 7a). However, the relationship between small intestinal length and net blood glucose flux is more complex (Figure 7b). As small intestinal length increases from 38 m to 45 m, there is a rise in blood glucose delivery since small intestinal starch digestion and glucose uptake capacity increase. However, further increases in intestinal length result in a sharp reduction in the release of glucose to the blood. This is explained by an increase in mucosal glucose oxidation beyond the supply arising from increased glucose availability due to starch and oligosaccharide hydrolysis. Despite evidence to suggest an overestimation of mucosal glucose requirement (Figure 4), this effect seems physiologically feasible. Indeed, although intestinal length is related to physiological state and body weight, the range for mature Holstein dairy cows has reported to be between 45 and 49 m (Gibb et al., 1992).

Pancreatic Amylase and SGLT1 Activity. Figure 8a presents the simple linear relationship between the maximum level of pancreatic secretion and starch digestibility. However, when examined against blood glucose flux (Figure 8b), an increasing rate of decline in blood glucose delivery is observed as maximum pancreatic fluid secretion is reduced. Again, the shift in starch hydrolysis and glucose uptake towards the ileum is responsible for this response. The overall low small intestinal digestibility of NSC is highlighted in the analysis of the effects of oligosaccharidase activity on model predictions (Figure 8c). The high rate of starch infusion used for simulation has demonstrated the overall imbalance between the capacity to hydrolyse starch

and for the removal of the products of starch hydrolysis. Oligosaccharidase is clearly a limiting factor for the applied level of starch infusion (4.5 kg starch/day), with a doubling in oligosaccharidase density producing a similar rate of increase in blood glucose appearance (Figure 8d). A similar impact on net blood glucose flux is achieved by raising maximum SGLT1 activity (Figure 8e). Hence, at this high rate of starch infusion, the processes associated with the unstirred water layer seem limiting as a whole. This implies that the diffusion of NSC, particularly oligosaccharide, across the UWL from the lumen is a crucial rate-limiting step in the recovery of glucose in the blood from digested starch.

Those parameters not shown in Figure 8 have little impact on model behaviour within the range tested. The GLUT2 transporter density ($v^{*}_{Ge,GeGb}$) only changed the net glucose flux when set at less than 40 μmol/cm^2/h, below which glucose accumulated in the enterocyte. The affinity of SGLT1 for glucose did not alter predictions of glucose uptake for the range tested (0.5 – 1.5 μmol). Likewise, the model was largely insensitive to changes in the affinity of oligosaccharidase ($M_{Ou,OuGu}$) (2.2 to 6.8 mmol/L).

DISCUSSION

A declining digestibility of starch in the small intestine of lactating dairy cows is evident at higher duodenal starch flows. Reynolds (2006) summarised data and observed a linear decrease of small intestinal digestion with duodenal starch flow (small intestinal starch digestion (g/kg duodenal starch flow) = 785 – 65.6 × duodenal starch flow (kg/d); Reynolds et al., 2014), as did Huntington et al. (2006). There have been several experiments conducted in the literature to elucidate the limits to starch digestion and glucose recovery. The conclusions of these studies have

537 differed depending on the nutritional regime examined together with the physiological state of the
538 cattle and the experimental technique utilised. Owens et al. (1986) reviewed the available data in
539 an attempt to clarify the points of control at which small intestinal starch digestion is limited in the
540 ruminant. They concluded that the enzymatic capacity did not limit intestinal starch digestion,
541 based on observations relating to total small intestinal starch disappearance. However, Owens et
542 al. (1986) also concluded that the influence of processing on particle size and starch granule
543 structure indicated a physical or physio-chemical barrier to carbohydrase activity. This was
544 confirmed by Larsen et al. (2009) who observed that rolling, compared with grinding, was
545 associated with a larger particle size, which reduced accessibility of enzymes and limited starch
546 digestion in the small intestine. The model does not account for the detailed effects of starch
547 particulate size on the rate of starch hydrolysis, unless this is represented by the estimate for the
548 digestion turnover time T_{SI}. In a study specifically aimed to investigate the effect of corn particle
549 size on starch digestion, Rémond et al. (2004) demonstrated a linear decline of 31% in small
550 intestinal starch digestion with mean particle size increasing from 0.7 to 3.7 mm. A similar effect
551 was demonstrated by Offner & Sauvant (2004) who found underprediction of rumen starch
552 digestion from in situ degradation characteristics when mean dietary particle size is less than
553 4mm. As small intestinal starch digestibility was negatively related to resistance to rumen
554 digestion, this would also mean an underpredicted small intestinal starch digestion. This may also
555 be important especially in the case of whole cereal grains for which reduced digestion can be
556 observed. However, a previous attempt at describing the effects of the physical characteristics of
557 starch on both ruminal and intestinal digestion proved largely unsatisfactory as a predictive tool
558 (Ewing and Johnson, 1987) with a lack of available data for parameterisation. In a more recent
559 comparison of starch digestion models, however, Patton et al. (2012) was able to demonstrate

potential for improved prediction by taking account of revised starch digestion rates to represent effects of starch source and processing. The ratio of amylose to amylopectin can, in theory at least, be related to starch digestion. Amylopectin may be more rapidly fermented than amylose, since amylopectin has a branched structure which exposes more non-reducing terminal glucose molecules for enzymatic attack than amylose. However, according to Philippeau et al. (1998) ruminal starch degradation was independent of the amylose:amylopectin ratio in starch.

Reynolds et al. (2014) and Mills et al. (1999b) both confirmed the observations of Owens et al. (1986) indicating no quantitative upper limit to postruminal starch disappearance. However, both Mills et al. (1999b) and Reynolds et al. (2014) highlight the potential for increasing compensatory large intestinal starch fermentation as total postruminal starch digestion increases. Larsen et al. (2009) demonstrated a higher contribution of the hind gut to (postrumen) starch digestion for legumes rich in protein with a lower total tract starch digestibility as compared to cereals. The inefficiencies of hind gut fermentation can negate the benefits of elevated small intestinal glucose absorption. Therefore, it is important to consider starch hydrolysis and glucose uptake by the small intestine rather than just starch disappearance prior to the ileo-caecal junction (Mills et al., 1999b). There is experimental evidence to suggest that increasing pancreatic secretion does increase small intestinal starch digestion, with the implication that amylase activity can be rate limiting (Castlebury and Preston, 1993; Taniguchi et al., 1995). Taniguchi et al. (1995) stimulated pancreatic secretion with abomasal casein infusion (120 g/d) and increased small intestinal starch digestion by almost 40% at the expense of large intestinal fermentation. Whether these observations are the result of increased proteolytic capacity leading to enhanced access of amylase to the starch granule or simply a result of increased amylolytic capacity is unclear. Indirect support for the importance of amylase activity on starch hydrolysis is found in the study

583 by Nozière et al. (2014) who found a 9% increase in rumen starch degradation when adding
584 exogenous amylase. Although still not support for any effect of amylolytic activity in the small
585 intestine, it is support of the sensitivity of starch hydrolysis for amylase activity. Consistently
586 good empirical relationships are found between rumen and small intestinal starch digestibility
587 (Nocek & Tamminga, 1991; Offner & Sauvant, 2004; Moharrery et al., 2014) but these
588 relationships do not take into account details such as amylase activity. Aiming to account for such
589 details (Mills et al., 1999) warranted the mechanistic approach adopted in the present study.

590 Other studies suggest that, instead of amylase activity, it is the capacity to absorb glucose
591 from hydrolysed starch that limits small intestinal glucose recovery by the cow (Cant et al., 1999).
592 Although Cant et al. (1999) did not infuse starch into the small intestine, they indicate that the
593 ability to upregulate glucose transport capacity was restricted to a level below that for other
594 species, where uptake capacity remains marginally in excess of requirement. Common TMR diets
595 that led to differences in amount of starch available in the small intestine did not regulate glucose
596 transporters (SGLT1 and GLUT2) (Lohrenz et al., 2011), and these authors postulated that it is
597 questionable if providing large amounts of rumen undegradable starch can modulate glucose
598 absorptive capacity in dairy cows under practical conditions. Therefore, absorption of glucose
599 during passage along the small intestine may limit postruminal digestive efficiency, irrespective of
600 enzymatic capacity. In a simulation of small intestinal starch digestion and glucose uptake,
601 Huntington (1997) suggested that the primary limitation to starch disappearance was enzymatic
602 capacity, unless more than 3 kg/d starch passes the duodenum, at which point SGLT1 transport
603 capacity becomes limiting. This 3 kg/d is below the maximum value of observed duodenal starch
604 flows used in reviews on small intestinal starch digestion (e.g., Reynolds et al., 2014). For
605 example, Moharrery et al. (2014) conclude that no limitation occurs up to 2 kg/d of duodenal

606 starch inflow. However, Offner & Sauvant (2004) do report a plateau for small intestinal starch
607 digestion with increasing inflow.

608 The previous simulation studies of Huntington (1997) and Cant et al. (1999) successfully
609 adopted a basal level of aggregation that considered luminal glucose uptake as a single stage
610 process. Hence, apparent affinity constants for glucose uptake by SGLT1 were uncorrected for the
611 effects of the UWL surrounding the microvilli. There are restrictions imposed with this
612 methodology since the potential for diffusion across the UWL and oligosaccharide hydrolysis
613 cannot be accounted for as independent limits to glucose uptake. The reductionist approach taken
614 in the present model allows for estimation of rate limiting processes and provides a tool for the
615 identification of novel methods of nutritional manipulation aimed at elevating the recovery of
616 duodenal starch as absorbed glucose. After careful evaluation, the model has potential for practical
617 application, especially when considered as part of a feed evaluation system incorporating a
618 mechanistic rumen model predicted duodenal starch inflow (e.g. Dijkstra et al., 1992). The ability
619 to vary starch hydrolysis rate and account explicitly for changing levels of pancreatic secretion are
620 particular strengths of the model, ultimately resulting in a predictive tool for starch digestion
621 rather than just glucose uptake under controlled conditions. Wider application of the model may
622 necessitate a more complete description of hydrolysis rates of different starches following
623 different degrees of processing (Theurer, 1986).

624 The behavioural analysis has shown that at high duodenal starch flows, most of the
625 parameters representing maximum rates of transport or hydrolysis are limiting to some extent.
626 This goes some way to explaining the apparent contradiction between published studies
627 identifying single rate limiting factors. This also corresponds with indications in literature that
628 there are limitations to small intestinal starch digestion (e.g. Offner & Sauvant, 2004). For

example, when the model is used to simulate the 3 levels of abomasal starch infusion by Kreikemeier et al. (1991), the effect of luminal starch flow can be clearly seen as a determinant of the pattern of starch appearance and disappearance along the small intestine. Figure 9a shows the elevation in luminal oligosaccharide flow distal from 50% of small intestinal length with the two highest rates of starch infusion (250, 375 mmol/h). The decline in oligosaccharide flow is much slower for the highest levels of starch infusion. As a result, the oligosaccharide load through the ileum is increased disproportionately. Since oligosaccharidase is relatively active in the ileal section, substantial quantities of glucose are produced in the UWL. The flow of glucose in the duodenum and jejunum section at low levels of starch entering the duodenum is small (Fig 9b). However, the ability of the brush border SGLT1 in the distal section of the ileum is limited. At high levels of starch entering the duodenum, a significant amount of glucose formed from oligosaccharides in the UWL diffuses to the lumen where it is lost via passage to the large intestine (up to 25 mmol/h, representing up to 10% of starch infused into the abomasum; Figure 9b). This type of analysis can be useful in diet evaluation, to prevent unnecessary outflow of glucose, oligosaccharides or starch to the large intestine, and to evaluate how appropriate actions can be taken such as reducing rumen escape starch, decreasing passage rate or increase the intrinsic digestibility of starch through feed processing. Recently, Gilbert et al. (2015) found evidence for a limitation of starch hydrolysis by maltase activity in the brush border of the small intestine of milk-fed calves. Similar limitations may occur in the adult ruminant. Simulation results in Figure 9 reiterate the need to coordinate enzymatic starch hydrolysis and intestinal glucose uptake, to maximise the efficiency of postruminal starch digestion for a given diet.

The present mechanistic model of small intestinal starch digestion and trans-epithelial glucose transport in dairy cattle provides insight into control points for maximising postruminal

carbohydrate digestive efficiency, and may be a useful tool for starch evaluation. Some limitations and weaknesses of the model that affect its prediction accuracy and precision have been identified. Firstly, data on metabolism at the brush border in high-producing dairy cattle were largely lacking, and this part of the model was partly parameterized using in vitro data and data from non-ruminants. The relative lack of data at brush border level indicates that this is an area where further research is required to improve the model. Moreover, microbial fermentation of starch in the small intestine was not represented. Secondly, the total contribution of glucose to enterocyte metabolism appears to be overestimated, especially in the presence of competing substrates such as glutamine. Thirdly, the model underestimated the contribution of paracellular diffusion of glucose from the digesta to the blood, particularly at high concentrations of luminal glucose. Finally, the model does not account for the detailed effects of starch particulate size on the rate of starch hydrolysis, unless this is represented by the estimate for the digestion turnover time as an input to the model.

The model predictions, combined with observations from the literature, would suggest a series of rate limiting steps is involved with small intestinal starch metabolism. The ideal situation is one where pancreatic fluid secretion is plentiful, the concentration of amylase in the fluid is high, oligosaccharide transport and hydrolysis are both non-limiting, with SGLT1 activity in excess of requirement. This situation will only exist for low levels of duodenal starch delivery. Beyond this, limitations will be imposed. The model has shown that these limits can be localised within a section of the small intestine (Figure 9a). However, spatial asynchrony between carbohydrase activity and transport capacity can amplify the effect of such localised limitations (Figure 9b) to affect the overall efficiency of small intestinal starch hydrolysis and glucose absorption.

CONCLUSIONS

This research suggests that there is no single factor that has the potential to limit starch digestion in the small intestine under conditions evaluated. The balance between small and large intestinal starch digestion is determined by a complex interplay of hydrolysis and transport processes, that themselves are dependent on diet and physiological state. The mechanistic approach adopted in the model provides for a more comprehensive quantitative understanding than has previously been available. Examination of the processes, ranging from duodenal starch delivery to glucose transport out of the enterocyte and NSC flow to the large intestine, as one complete system is particularly beneficial. Such an approach avoids undue emphasis on certain potentially rate limiting steps and the oversight of others. The mechanistic model of small intestinal starch digestion and transepithelial glucose transport is a useful tool for feed evaluation especially where substantial quantities of starch flow undegraded from the rumen. The model also provides an insight into control points for maximising postruminal carbohydrate digestive efficiency.

ACKNOWLEDGEMENTS

The authors thank Dr C. K. Reynolds, University of Reading, for providing helpful suggestions and other intellectual input during the conduct of this research. Funding was obtained in part from the Canada Research Chairs program (National Science and Engineering Council,

Ottawa). The contribution of André Bannink and Jan Dijkstra was partly funded by the Product Board Animal Feed (Zoetermeer, the Netherlands).

REFERENCES

Armstrong, D. G., and D. E. Beever. 1969. Post-abomasal digestion of carbohydrate in the ruminant animal. Pages 121-131 in Proc. Nutr. Soc. 28.

Bauer, M. L. 1996. Nutritional regulation of small intestinal glucose absorption in ruminants. [Ph.D. Dissertation]. University of Kentucky, Lexington.

Bauer, M. L., D. L. Harmon, D. W. Bohnert, A. F. Branco, and G. B. Huntington. 1997. Influence of a-linked glucose on sodium-glucose cotransport activity along the small intestine in cattle. J. Anim. Sci. 75(Suppl 1):263.

Bauer, M.L., D. L. Harmon, K. R. McLeod, and G. B. Huntington. 1995. Adaptation to small intestinal starch assimilation and glucose transport in ruminants. J. Anim. Sci. 73:1828-1838.

Bibby, J., and H. Toutenburg. 1977. Prediction and Improved Estimation in Linear Models. John Wiley & Sons, London, UK.

Braun, U., O. Marmier, and N. Pusterla. 1995. Ultrasonographic examination of the small intestine of cows with ileus of the duodenum, jejunum or ileum. Veterinary Record 137:209-215.

Breves, G., and S. Wolffram. 2006. Transport systems in the epithelia of the small and large intestines. Pages 139–154 in Ruminant Physiology: Digestion, Metabolism and Impact of Nutrition on Gene Expression, Immunology and Stress. K. Sejrsen, T. Hvelplund, and M. O. Nielsen, ed. Wageningen Academic Publishers, Wageningen, the Netherlands

720 Burant, C. F., W. I. Sivitz, H. Fukumoto, T. Kayano, S. Nagamatsu, S. Seino, J. E. Pessin, and G.
721 I. Bell. 1991. Mammalian glucose transporters: structure and molecular regulation. Rec.
722 Prog. Horm. Res. 47:349-388.
723 Cant, J. P, P. H. Luimes, T. C. Wright, and B. W. McBride. 1999. Modeling intermittent digesta
724 flow to calculate glucose uptake capacity of the bovine small intestine. Am. J. Physiol.
725 276:G1442-G1451.
726 Castlebury, R. E., and R. L. Preston. 1993. Effect of dietary protein level on nutrient digestion in
727 lambs duodenally infused with corn starch. J. Anim. Sci. 71: 264(Abstract)
728 Cheeseman, C. I., and B. Harley. 1991. Adaptation of glucose transport across rat enterocyte
729 basolateral membrane in response to altered dietary carbohydrate intake. J. Physiol.
730 437:563-575.
731 Cheeseman, C. I., and D. D. Maenz. 1989. Rapid regulation of D-glucose transport in basolateral
732 membrane of rat jejunum. Am. J. Physiol. 256:G878-G883.
733 Cone, J. W. 1991. Degradation of starch in feed concentrates by enzymes, rumen fluid and rumen
734 enzymes. J. Sci. Food Agric. 54:23-34.
735 Coombe, N. B., and R. C. Siddons. 1973. Carbohydrases of the bovine small intestine. Br. J. Nutr.
736 30:269-276.
737 Croom, W. J., L. S. Bull, and I. L. Taylor. 1992. Regulation of pancreatic exocrine secretion in
738 ruminants: A review. J. Nutr. 122:191-202.
739 Diamond, J. M., and W. H. Karasov. 1987. Adaptive regulation of intestinal nutrient transporters.
740 Proc. Nat. Acad. Sci, USA 84:2242-2245.
741 Dijkstra, J., H. D. StC. Neal, D. E. Beever, and J. France. 1992. Simulation of nutrient digestion,
742 absorption and outflow in the rumen: model description. J. Nutr. 122:2239-2256.

743 Dyer, J., S. Vayro, T. P. King, and S. P. Shirazi-Beechey. 2003. Glucose sensing in the intestinal
744 epithelium. Eur. J. Biochem. 270:3377–3388.
745 Eggermont, E. 1969. The hydrolysis of the naturally occurring a-glucosides by the human
746 intestinal mucosa. Eur. J. Biochem. 9:483.
747 Ewing, D. L., and D. E. Johnson. 1987. Corn particle starch digestion, passage and size reduction
748 in beef steers: a dynamic model. J. Anim. Sci. 64:1194-1204.
749 Ferraris, R. P., S. Yasharpour, K. C. Kent Lloyd, R. Mirzayan, and J. M. Diamond. 1990. Luminal
750 glucose concentrations in the gut under normal conditions. Am. J. Physiol. 259:G822-
751 G837.
752 Fushiki, T., and K. Iwai. 1989. Two hypotheses on the feedback regulation of pancreatic enzyme
753 secretion. FASEB J. 3:121-126.
754 Gibb, M. J., W. E. Ivings, M. S. Dhanoa, and J. D. Sutton. 1992. Changes in the body components
755 of autumn-calving Holstein-Friesian cows over the first 29 weeks of lactation. Anim. Prod.
756 55:339-360.
757 Gilbert, M. S., A. J. Pantophlet, H. Berends, A. M. Pluschke, J. J. G. C. van den Borne, W. H.
758 Hendriks, H. A. Schols, and W. J. J., Gerrits. 2015. Fermentation in the small intestine
759 contributes substantially to intestinal starch disappearance in calves. J. Nutr. 145:1147-
760 1155.
761 Gill, M., J. France, M. Summers, B. W. McBride, and L. P. Milligan. 1989. Simulation of the
762 energy costs associated with protein turnover and Na^+, K^+ -transport in growing lambs. J.
763 Nutr. 119:1287-1299.
764 Hanson, P. J., and D. S. Parsons. 1977. Metabolism and transport of glutamine and glucose in
765 vascularly perfused rat small intestine. Biochem. J. 166:509-519.

766 Harmon, D. L. 1993. Nutritional regulation of postruminal digestive enzymes in ruminants. J.
767 Dairy Sci. 76:2102-2111.
768 Hatew, B., Bannink, A., van Laar, H., de Jonge, L. H., and Dijkstra, J. 2016. Increasing harvest
769 maturity of whole-plant corn silage reduces methane emission of lactating dairy cows. J.
770 Dairy Sci. 99:354-368.
771 Hediger, M. A., and D. B. Rhoads. 1994. Molecular physiology of sodium-glucose cotransporters.
772 Physiol. Rev. 74:993-1026.
773 Huntington, G. B.1997. Starch utilization by ruminants: From basics to the bunk. J. Anim. Sci.
774 75:852-867.
775 Huntington, G. B., D. L. Harmon, and C. J. Richards. 2006. Sites, rates, and limits of starch
776 digestion and glucose metabolism in growing cattle. J. Anim. Sci. 84(E. Suppl.):E14-E24.
777 Huntington, G. B., and P. J. Reynolds. 1986. Net absorption of glucose, L-lactate, volatile fatty
778 acids, and nitrogenous compounds by bovine given abomasal infusions of starch or
779 glucose. J. Dairy Sci. 69:2428-2436.
780 Janes, A. N., T. E. C. Weekes, and D. G. Armstrong. 1985. Carbohydrase activity in the pancreatic
781 tissue and small intestine mucosa of sheep fed dried grass or corn based diets. J. Agric. Sci.
782 (Camb.) 104:435-443.
783 Keller, P. J., E. Cohen, and H. Neurath.1958. The proteins of pancreatic juice. J. Biol. Chem.
784 233:344-349.
785 Kellett, G. L., and P. A. Helliwell. 2000. The diffusive component of intestinal glucose absorption
786 is mediated by the glucose-induced recruitment of GLUT2 to the brush-border membrane.
787 Biochem. J. 350:155-162.

788 Khan, N. A., P. Q. Yu, M. Ali, J. W. Cone, and W. H. Hendriks. 2015. Nutritive value of corn
789 silage in relation to dairy cow performance and milk quality. J. Sci. Food Agric. 95:238-
790 252.
791 Khorasani, G. R., W. C. Sauer, L. Ozimek, and J. J. Kennelly. 1990. Digestion of soybean meal
792 and canola meal protein and amino acids in the digestive tract of young ruminants. J.
793 Anim. Sci. 68:3421-3428.
794 Krehbiel, C. R., R. A. Britton, D. L. Harmon, J. P. Peters, R. A. Stock, and H. E. Grotjan. 1996.
795 Effects of varying levels of duodenal or midjejunal glucose and 2-deoxyglucose infusion
796 on small intestinal disappearance and net portal glucose flux in steers. J. Anim. Sci.
797 74:693-700.
798 Kreikemeier, K. K., and D. L. Harmon. 1995. Abomasal glucose, corn starch and corn dextrin
799 infusions in cattle: Small intestinal disappearance, net portal glucose flux and ileal
800 oligosaccharide flow. Br. J. Nutr. 73:763-772.
801 Kreikemeier, K. K., D. L. Harmon, R. T. Brandt, T. B. Avery, and D. E. Johnson. 1991. Small
802 intestinal starch digestion in steers: Effect of various levels of abomasal glusose, corn
803 starch and corn dextrin on small intestinal disappearance and net glucose absorption. J.
804 Anim. Sci. 69:328-338.
805 Kreikemeier, K. K., D. L. Harmon, J. P. Peters, K. L. Gross, C. K. Armendariz, and C. R.
806 Krehbiel. 1990. Influence of dietary forage and feed intake on carbohydrase activities and
807 small intestinal morphology of calves. J. Anim. Sci. 68:2916-2929.
808 Krstic, R.V. 1979. Ultrastucture of the Mammalian Cell. Springer-Verlag, Berlin.
809 Larsen, M., P. Lund, M. W. Weisbjerg, and T. Hvelplund. 2009. Digestion site of starch from
810 cereal and legumes in lactating cows. Anim. Feed Sci. Technol. 153:236-248.

811 Largis, E. E., and F. A. Jacobs. 1971. Effects of phlorizin on glucose transport in blood and
812 lymph. Biochimica et Biophysica Acta 225:301.
813 Lennox, A. M., and G. A. Garton. 1968. The absorption of long-chain fatty acids from the small
814 intestine of the sheep. Br. J. Nutr. 2:247-254.
815 Levitt, M. D., A. Strocchi, and D. G. Levitt. 1992. Human jejunal unstirred layer: evidence for
816 extremely efficient luminal stirring. Am. J. Physiol. 262:G593-G596.
817 Li, S., E. Khafipour, D. O. Krause, A. Kroeker, J. C. Rodriguez-Lecompte, G. N. Gozho, and J. C.
818 Plaizier. 2012. Effects of subacute ruminal acidosis challenges on fermentation and
819 endotoxins in the rumen and hindgut of dairy cows. J. Dairy Sc. 95:294-303.
820 Lohrenz, A. K., K. Duske ,U. Schönhusen , B. Losand , H. M. Seyfert , C. C. Metges , and H. M.
821 Hammon. 2011. Glucose transporters and enzymes related to glucose synthesis in small
822 intestinal mucosa of mid-lactation dairy cows fed 2 levels of starch. J. Dairy Sci. 94:4546-
823 4555.
824 Lucas, M. 1983. Determination of acid surface pH in vivo in rat proximal jejunum. Gut 24:734-
825 739.
826 MacRae, J.C. 1967. Ph.D. Thesis. The University of Newcastle upon Tyne.
827 Madge, D. S. 1975. The Mammalian Alimentary System: A Functional Approach, Edward
828 Arnold, London.
829 Maenz, D. D., and C. I. Cheeseman.1987. The Na^+-independent D-glucose transporter in the
830 enterocyte basolateral membrane. J. Membr. Biol. 97:259-266.
831 McCarthy, R. D., T. H. Klusmeyer, J. L. Vicini, J. H. Clark, and D. R. Nelson. 1989. Effects of
832 source of protein and carbohydrate on ruminal fermentation and passage of nutrients to the
833 small intestine of lactating cows. J. Dairy Sci. 72:2002-2016.

834 Meddings, J. B., and H. Westergaard. 1989. Intestinal glucose transport using in vivo perfused rat
835 jejunum: model analysis and derivation of corrected kinetic constants. Clin. Sci. Lond.
836 76:403-413.
837 Mills, J. A. N., L. A. Crompton, J. L. Ellis, J. Dijkstra, A. Bannink, S. Hook, C. Benchaar, J.
838 France. 2014. A dynamic mechanistic model of lactic acid metabolism in the rumen. J.
839 Dairy Sci. 97:2398-2414.
840 Mills, J. A. N., J. France, and J. Dijkstra. 1999a. A review of starch digestion in the lactating dairy
841 cow and proposals for a mechanistic model: 1. Dietary starch characterisation and ruminal
842 starch digestion. J. Anim. Feed Sci. 8:291-340.
843 Mills, J. A. N., J. France, and J. Dijkstra. 1999b. A review of starch digestion in the lactating dairy
844 cow and proposals for a mechanistic model: 2. Postruminal starch digestion and small
845 intestinal glucose absorption. J. Anim. Feed Sci. 9:451-481.
846 Mills, J. A. N., L. A. Crompton, J. L. Ellis, J. Dijkstra, A. Bannink, S. Hook, C. Benchaar, and J.
847 France. 2014. A dynamic mechanistic model of lactic acid metabolism in the rumen. J.
848 Dairy Sci. 97:2398-2414.
849 Mitchell and Gauthier Associates. 1995. Advanced Continuous Simulation Language (ACSL).
850 User's guide / Reference manual. version 11.
851 Moharrery, A., M. Larsen, and M. R. Weisbjerg. 2014. Starch diegstion in the rumen, small
852 intestine, and hind gut of dairy cows - A meta-analysis. Anim. Feed Sci. Technol. 192:1-
853 14.
854 Nocek, J. E., and S. Tamminga. 1991. Site of digestion of starch in the gastrointestinal tract of
855 dairy cows and its effect on milk yield and composition. J. Dairy Sci. 74:3598-3629.

856 Offner, A., and D. Sauvant. 2002. Prediction of in vivo starch digestion in cattle from in situ data.
857 Animal Feed Science & Technology 111:41-56.
858 Okine, E. K., and D. R. Glimm, J. R. Thompson and J. J. Kennelly. 1995. Influence of stage of
859 lactation on glucose and glutamine metabolism in isolated enterocytes from dairy cattle.
860 Metab. 44:325-331.
861 Owens, F. N., R. A. Zinn, and Y. K. Kim. 1986. Limits to starch digestion in the ruminant small
862 intestine. J. Anim. Sci. 63:1634-1648.
863 Pappenheimer, J. R., and K. Z. Reiss. 1987. Contribution of solvent drag through intercellular
864 junctions to absorption of nutrients by the small intestine of the rat. J. Mem. Biol. 100:123-
865 136.
866 Patton, R. A., J. R. Patton, and S. E. Boucher. 2012. Defining ruminal and total-tract starch
867 degradation for adult dairy cattle using in vivo data. J. Dairy Sci. 96:765-782.
868 Peyrat, J., R. Baumont, A. le Morvan, and P. Nozière. 2016. Effect of maturity and hybrid on
869 ruminal and intestinal digestion of corn silage in dairy cows. J. Dairy Sci. 99:258-268.
870 Philippeau, C., J. Landry, and B. Michalet-Doreau. 1998. Influence of the Biochemical and
871 Physical Characteristics of the Maize Grain on Ruminal Starch Degradation. J Agric
872 Food Chem 46, 4287-4291.
873 Pierzynowski, S. G. 1986. The secretion of pancreatic juice in sheep in different fed treatments.
874 Polskie Archiwum Weterynaryjne 26:31-39.
875 Pierzynowski, S. G. 1989. Exocrine pancreatic function in calves fed liquid or solid food. Asian J.
876 Anim. Sci. 2:179-180.

877 Pierzynowski, S. G., W. Barej, M. Mikolajczyk, and R. Zabielski. 1988. The influence of light
878 fermented carbohydrates on the exocrine pancreatic secretion in cows. J. Anim. Physiol.
879 Anim. Nutr. 60:234-238.
880 Rémond, D., J. L. Cabrera-Estrada, M. Champion, B. Chauveau, R. Coudre, and C. Poncet. 2004.
881 Effect of corn particle size on site and extent of starch digestion in lactating dairy cows. J.
882 Dairy Sci. 87:1389-1399.
883 Reynolds, C. K. 2006. Production and metabolic effects of site of starch digestion in lactating
884 dairy cattle. Anim. Feed Sci. Technol. 130:78-94.
885 Reynolds, C. K., D. J. Humphries, A. M. Van Vuuren, J. Dijkstra, and A. Bannink. 2014.
886 Considerations for feeding starch to high yielding dairy cows Pages 27-47 in Recent
887 Advances in Animal Nutrition 2014. P. C. Garnsworthy, J. Wiseman, ed. Context Products
888 Ltd, Packington, UK.
889 Reynolds, C. K., and G. B. Huntington. 1988. Partition of portal-drained visceral net flux in beef
890 steers. 1. Blood flow and net flux of oxygen, glucose and nitrogenous compounds across
891 stomach and post-stomach tissues. Br. J. Nutr. 60:539-551.
892 Reynolds, C. K., G. B. Huntington, and P. J. Reynolds. 1988. Net portal-drained visceral and
893 hepatic metabolism of glucose, L-lactate and nitrogenous compounds in lactating Holstein
894 cows. J. Dairy Sci. 71:1803-1812.
895 Reynolds, C. K., H. F. Tyrrell, and P. J. Reynolds. 1991. Effects of diet forage-to-concentrate ratio
896 and intake on energy metabolism in growing beef heifers: net nutrient metabolism by
897 visceral tissues. J. Nutr. 121:1004-1015.
898 Rosenblum, J. L., C. L. Irwin, and D. H. Alpers. 1988. Starch and glucose oligosaccharides protect
899 salivary-type amylase activity at acid pH. Am. J. Physiol. 254:G775-G780.

900 Ruckebusch, Y. 1988. Motility of the gastrointestinal tract. Page 64 in The Ruminant Animal. D.
901 C. Church, ed. 64 Prentice Hall, Englewood Cliffs, New Jersey.
902 Russell, J. R., A. W. Young, and N. A. Jorgensen. 1981. Effect of dietary corn starch intake on
903 pancreatic amylase and intestinal maltase and pH in cattle. J. Anim. Sci. 52:1177-1182.
904 Shirazi-Beechey, S. P., B. A. Hirayama, Y. Wang, D. Scott, M. W. Smith, and E. M. Wright.
905 1991. Ontogenic development of lamb intestinal sodium-glucose co-transporter is
906 regulated by diet. J. Physiol. 437:699-708.
907 Shirazi-Beechey, S. P., I. S. Wood, J. Dyer, D. Scott, and T. P. King. 1995. Chapter 5. Intestinal
908 sugar transport in ruminants. Pages 117-133 in Ruminant Physiology: Digestion,
909 Metabolism, Growth and Reproduction: Proceedings of the 8th International Symposium
910 on Ruminant Physiology. W. V. Engelhardt, S. Leonhard-Marek, G. Breves, D. Giesecke,
911 ed. Ferdinand Enke Verlag, Stuttgart.
912 Siddons, R. C. 1968. Carbohydrase activities in the bovine digestive tract. Biochem. J. 108:839-
913 844.
914 Stevens, B. R. 1992. Chapter 10. Amino Acid Transport in Intestine. Pages 149-163 in
915 Mammalian Amino Acid Transport. Mechanisms and Control. M. S. Kilberg, D.
916 Haussinger ed. Plenum Press, New York.
917 Stryer, L. 1995. Biochemistry, 4th edition. W.H. Freeman and Company, New York.
918 Taniguchi, K., G. B. Huntington, and B. P. Glenn. 1995. Net nutrient flux by visceral tissues of
919 beef steers given abomasal and ruminal infusions of casein and starch. J. Anim. Sci.
920 73:236-249.
921 Theurer, C. B. 1986. Grain processing effects on starch utilization by ruminants. J. Anim. Sci.
922 63:1649-1662.

923 Thorens, B. 1993. Facilitated glucose transporters in epithelial cells. Ann. Rev. Physiol. 55:591-
924 608.
925 Waldo, D. R. 1973. Extent and partition of cereal grain starch digestion in ruminants. J. Anim. Sci.
926 37:1062-1074.
927 Walker, J. A., and D. L. Harmon. 1995. Influence of ruminal or abomasal starch hydrolysate
928 infusion on pancreatic exocrine secretion and blood glucose and insulin concentrations in
929 steers. J. Anim. Sci. 73:3766-3774.
930 Walker, J. A., C. R. Krehbiel, D. L. Harmon, G. St. Jean, W. J. Croom, and W. M. Hagler. 1994.
931 Effects of slaframine and 4-diphenylacetoxy-N-methylpiperidine methiodide (4DAMP) on
932 pancreatic exocrine secretion in the bovine. Can. J. Physiol. Pharm. 72:39-44.
933 Windmueller, H. G. 1982. Glutamine utilisation by the small intestine. Adv. Enz. 53:201-237.
934 Windmueller, H. G., and A. E. Spaethe. 1974. Uptake and metabolism of plasma glutamine by the
935 small intestine. J. Biol. Chem. 249:5070-5079.
936 Zhao, F., E. K. Okine, C. I. Cheeseman, S. P. Shirazi-Beechey, and J. J. Kennelly. 1998. Glucose
937 transporter gene expression in lactating bovine gastrointestinal tract. J. Anim. Sci.
938 76:2921-2929.
939

Table 1. Parameter values*†.

Transaction	M_{ijk}	$M_{\mathrm{NSC}jk}$	v^{*}_{ijk}	v^{**}_{ijk}	$v^{(\mathrm{o})}_{ijk}$	θ_{ijk}	$k^{(d)}_{ijk}$	Y_{ijk}	T^{*}_{Sl}
GbGe	0.048	0.075	4.88E-5	1.22E-5					
GbGu							0.0242		
GeGb	0.023	0.075	4.88E-5	1.22E-5		5.0			
GlGu							0.0242		
GuGb							0.0242		
GuGe	1.0E-4	0.075	2.92E-4	7.3E-7		5.0			
GuGl							0.0242		
OlOu							0.0089		
OuGu	0.0045		6.0E-5		6.0	0.19		0.9	
OuOl							0.0089		
PfAl	0.21		22000	5000		3.0			
PfPp								11.9	
PpAl	2.5		8.0E-4	3.0E-4		15.0			
SlOl	0.0216		6.0E-5		6.9	0.6			11.8

*See Appendix for explanation of notation

† N.B. Parameters relating to small intestinal physiology are considered as input parameters, subject to variation dependent on animal type, and are not displayed here but are discussed in the text.

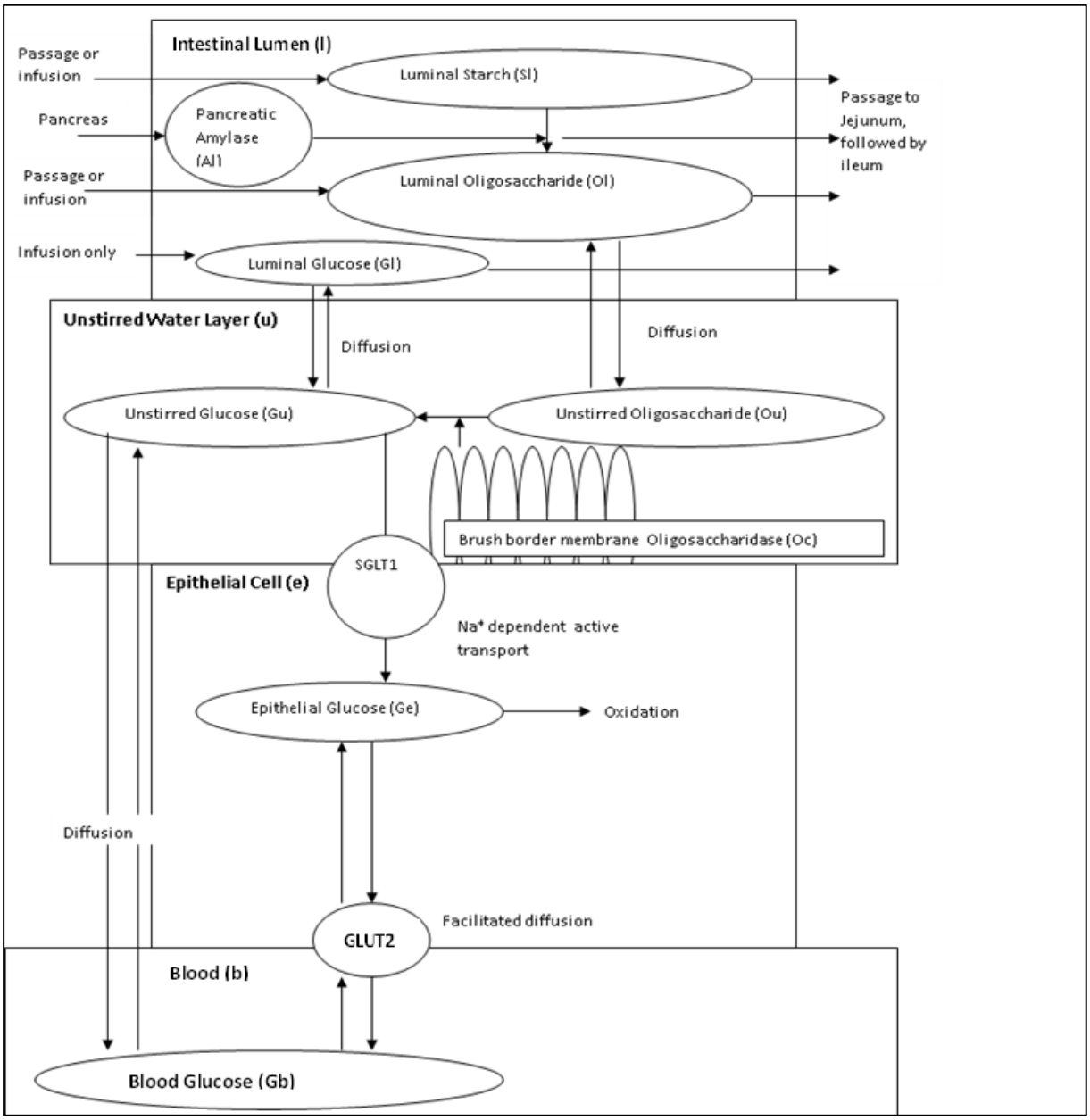

Figure 1. Diagrammatic representation of one sub-section in the small intestine model.

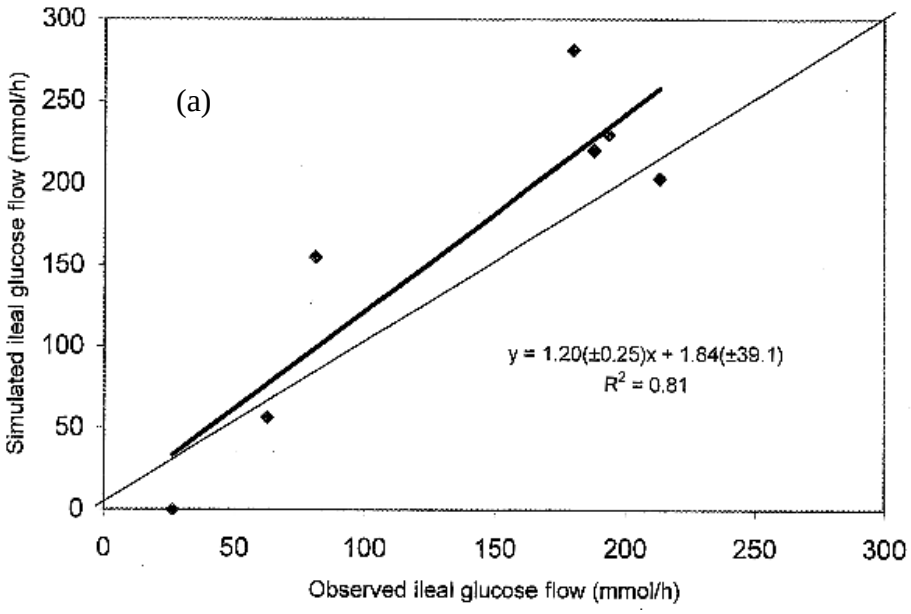

965

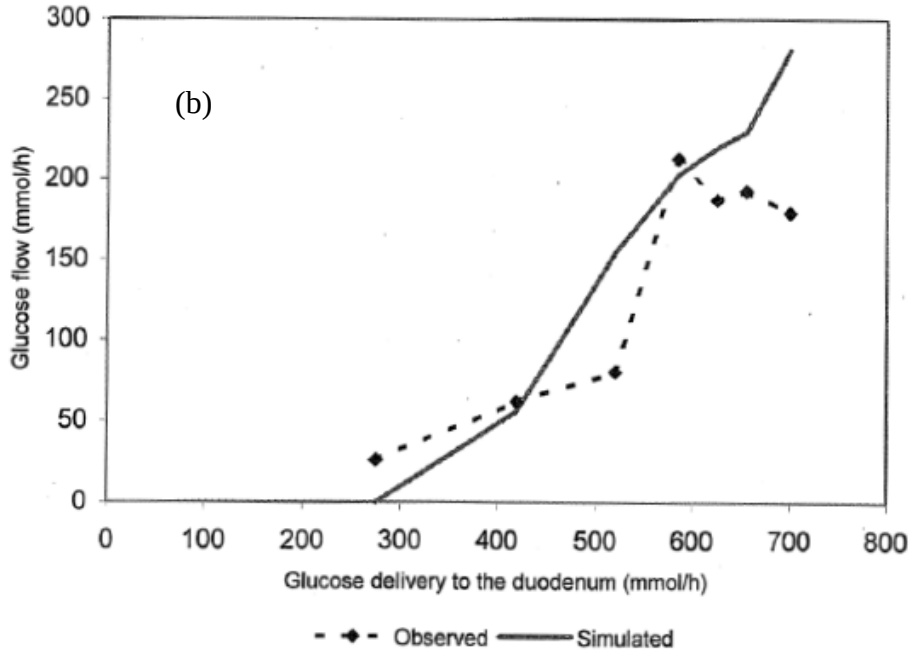

966

967 **Figure 2**. Observed and simulated ileal glucose flow in dairy heifers infused with glucose at the
968 duodenum. (a) regression [root Mean Square Prediction Error (RMSPE) = 38.6% of observed
969 mean, bias of prediction = 20.7% of MSPE, error due to regression = 39.3%, disturbance
970 proportion = 40.0%], (b) flows.

971

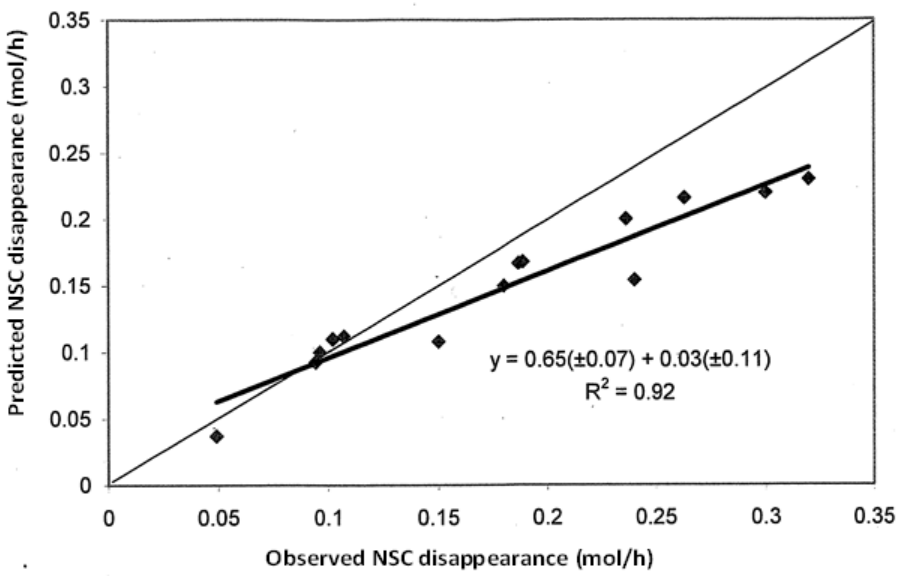

Figure 3. Regression of observed and predicted non-structural carbohydrate (NSC) disappearance in the small intestine. root Mean Square Prediction Error (RMSPE)= 25.4%, bias of prediction = 45.2% of MSPE, error due to regression = 25.1%, disturbance proportion = 29.7%.

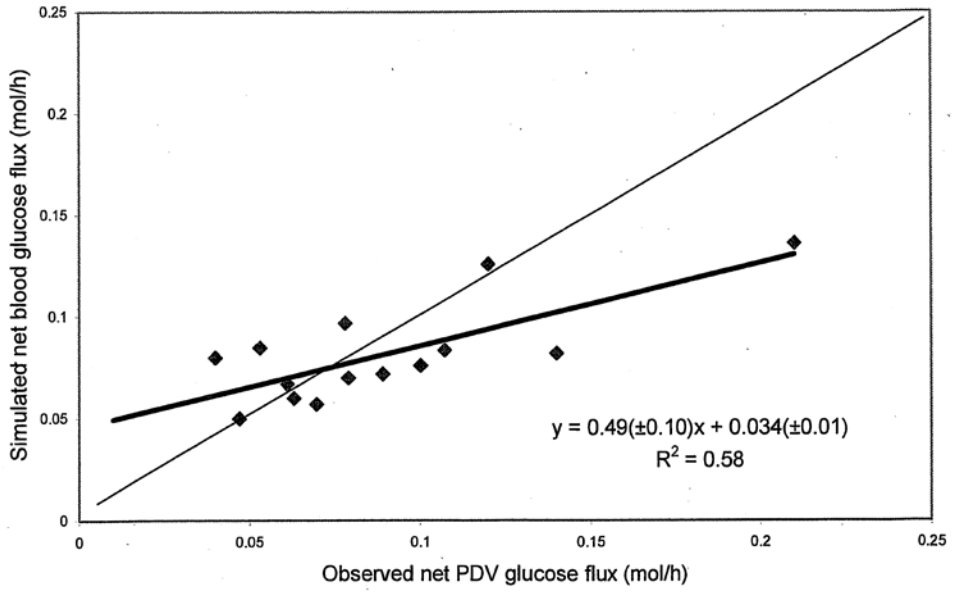

980

981 **Figure 4**. A comparison of observed net portal drained visceral (PDV) glucose flux and simulated

982 net glucose release from the small intestinal epithelial tissue.

983

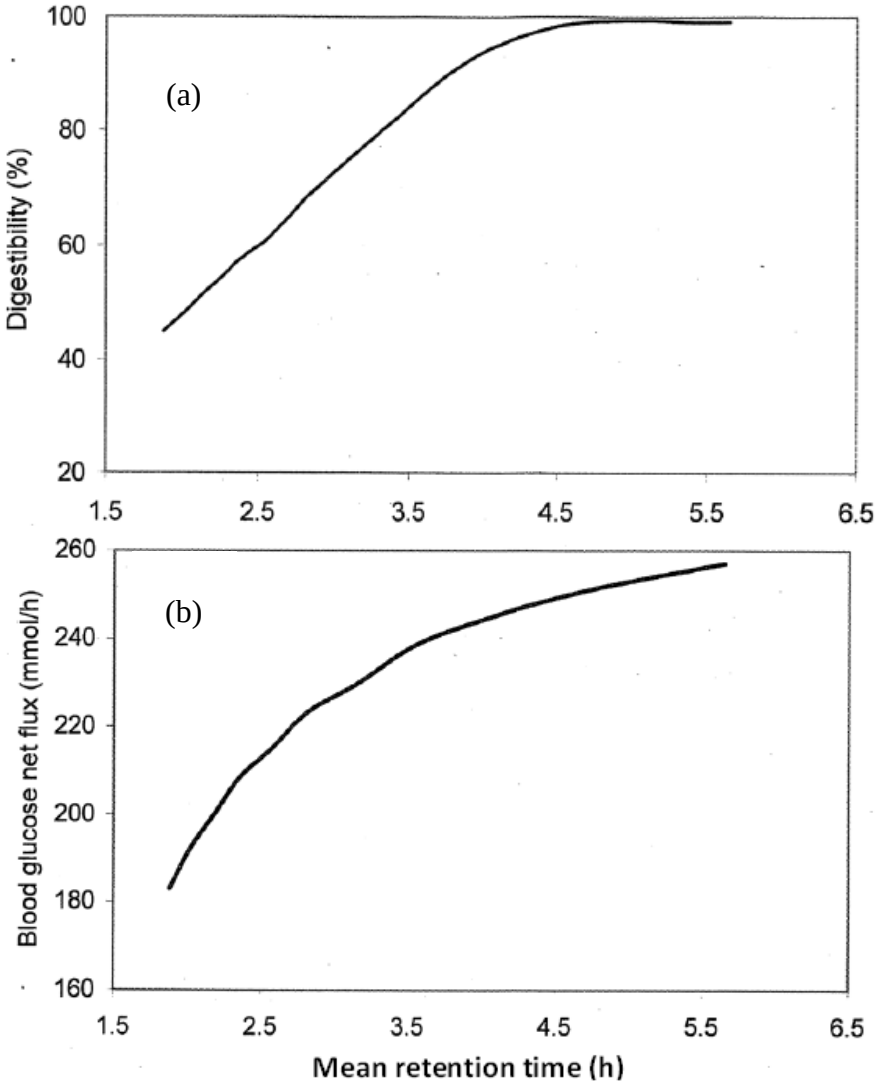

Figure 5. Small intestinal starch flow. (a) simulated relationship between starch digestibility and mean retention time (MRT), (b) simulated net blood glucose flux and MRT.

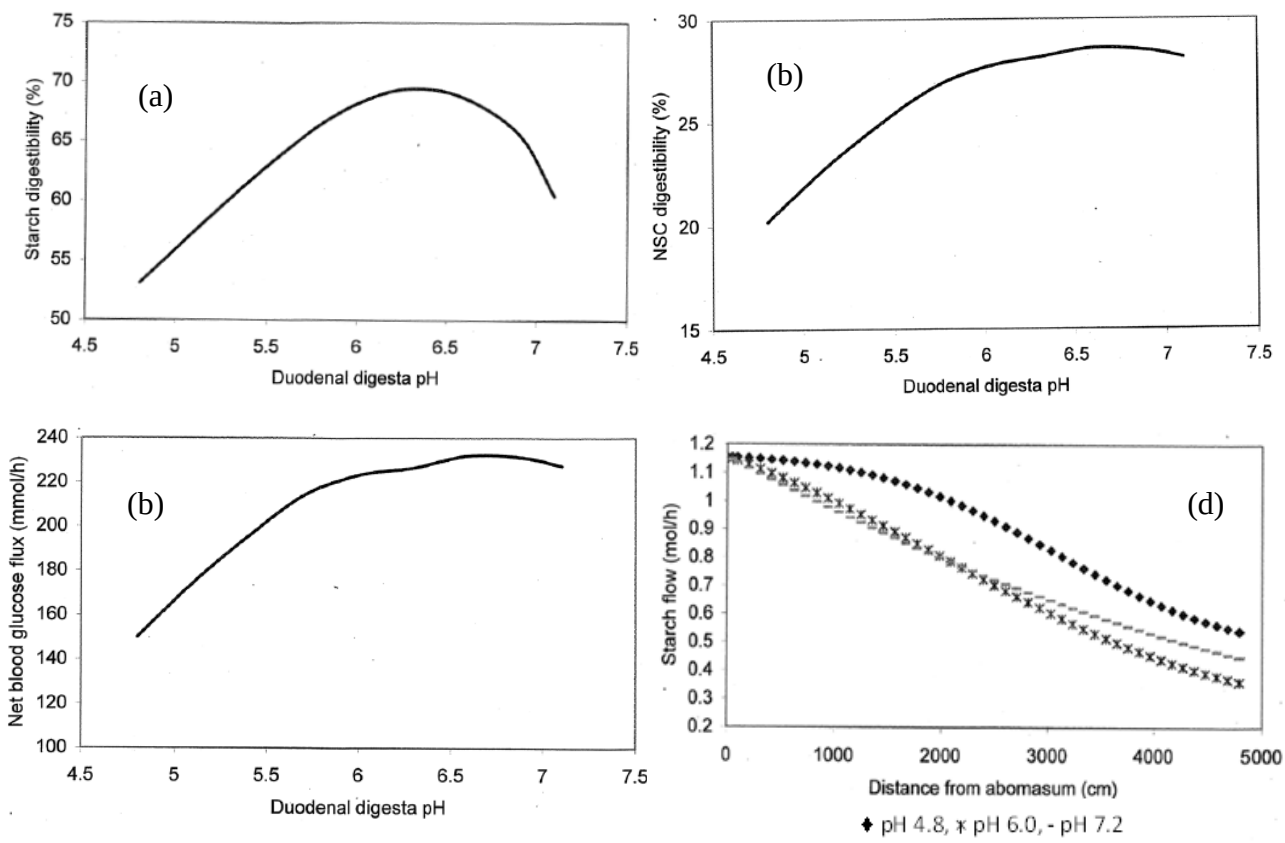

Figure 6. Luminal pH. (a) simulated starch digestibility over a range of duodenal digesta pH, (b) simulated non-structural carbohydrate (NSC) digestibility over a range of duodenal digesta pH, (c) duodenal digesta pH and net blood glucose flux, (d) duodenal digesta pH and starch flow down the small intestine.

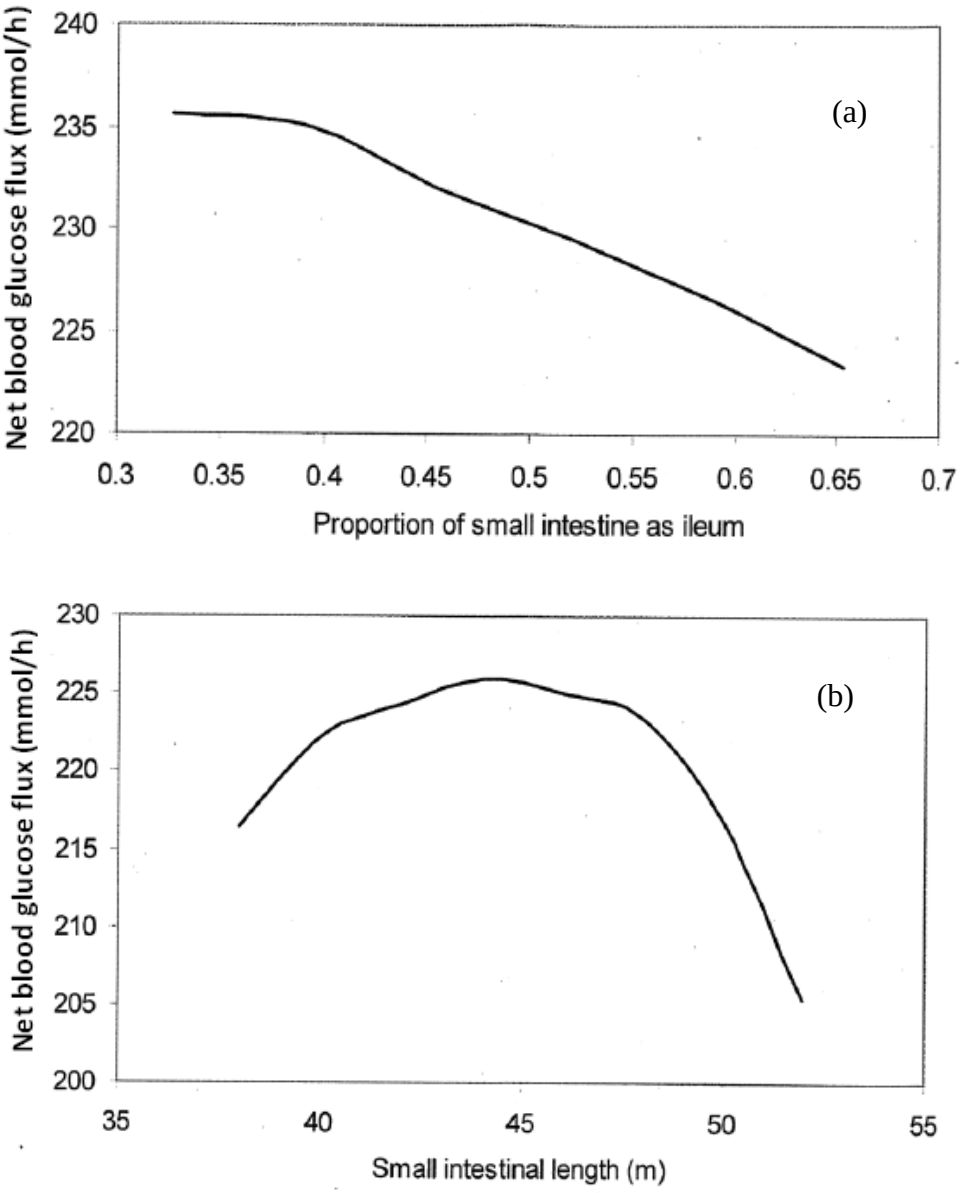

Figure 7. Intestinal physiology. (a) net blood glucose flux and proportion of small intestine defined as ileum, (b) small intestinal length and net blood glucose flux.

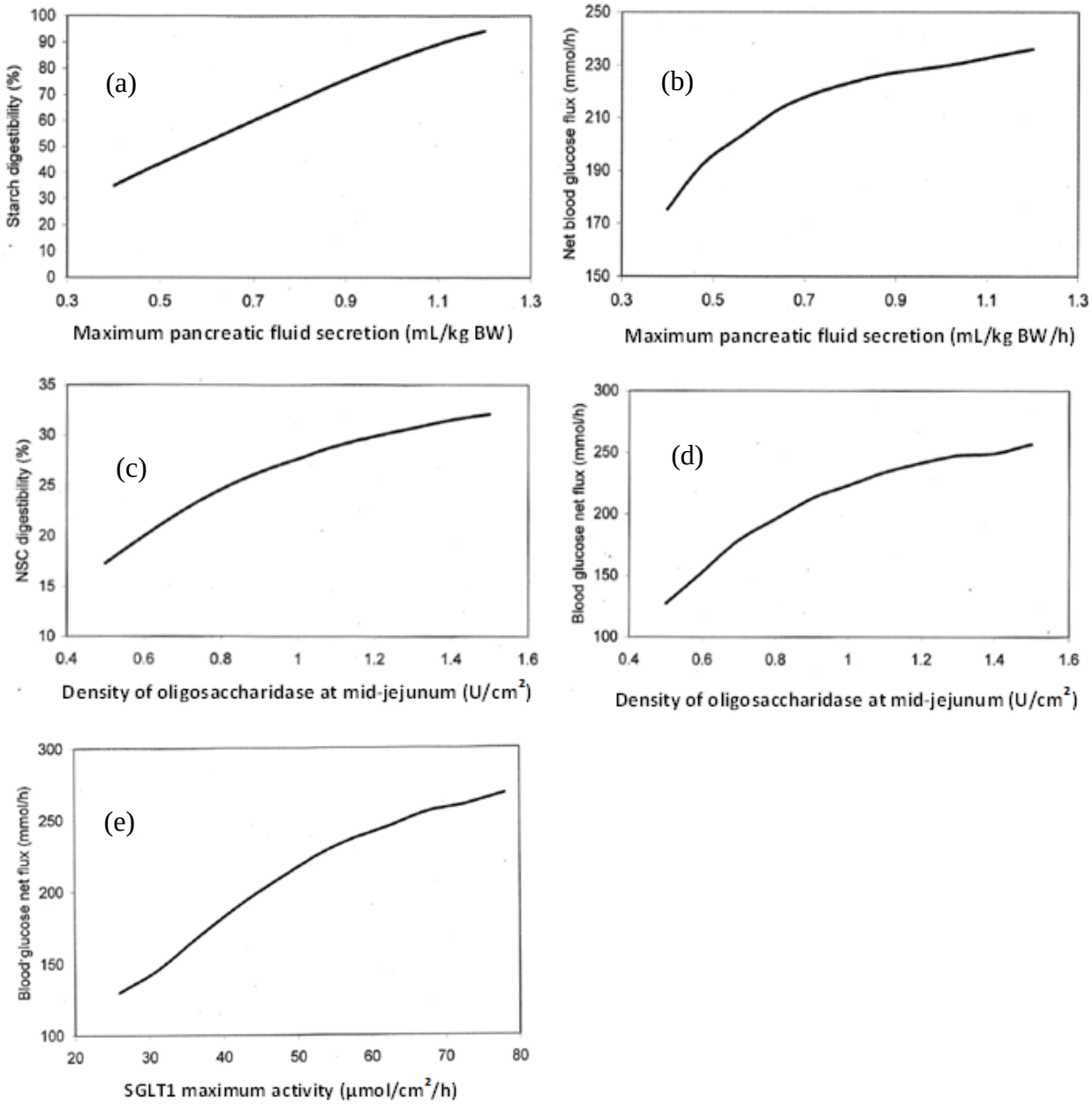

Figure 8. Pancreatic amylase and SGLT1 activity. (a) maximum rate of pancreatic fluid secretion and starch digestibility, (b) maximum rate of pancreatic fluid secretion and net blood glucose flux, (c) non-structural carbohydrate (NSC) digestibility and maximum oligosaccharidase activity, (d) response of blood glucose net flux to density of oligosaccharidase at the unstirred water layer, (e) simulated net blood glucose flux and SGLT1 maximum activity.

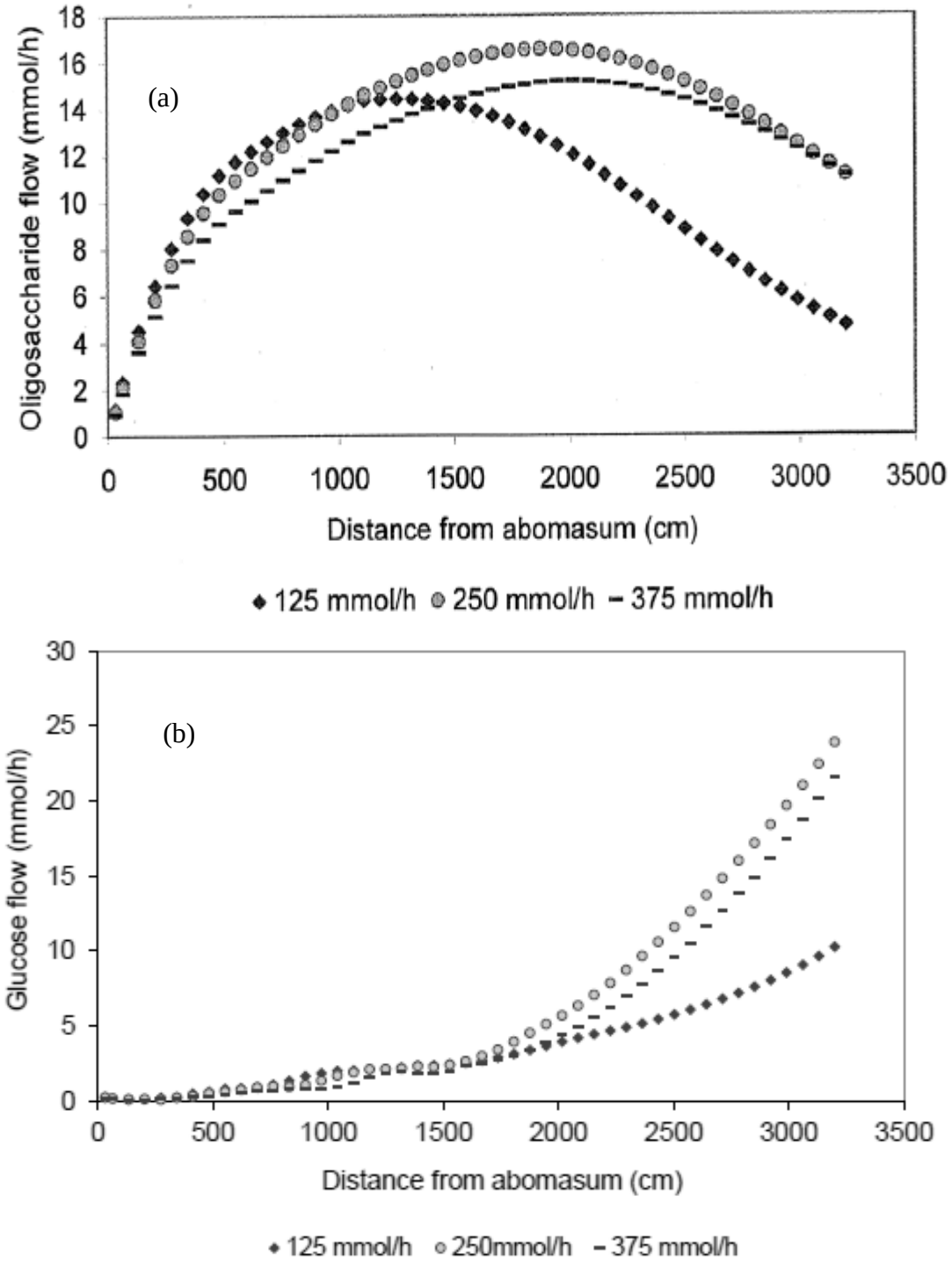

Figure 9. Simulated flow during passage along the small intestine in steers infused with increasing levels of starch into the abomasum. (a) oligosaccharide, (b) glucose.

Appendix: Mathematical Model Statements*

Duodenal Lumen

Amylase in Lumen, Q_{Al} mol

Concentration:

$$C_{Al} = Q_{Al} / V_{Lu} \quad (1.1)$$

Inputs:

$$P_{Al,PfAl} = Y_{Pp,PfPp} Y_{Al,PpAl} U_{Pf,PfAl} \quad (1.2)$$

Outputs:

$$U_{Al,AlEx} = k_p Q_{Al} \quad (1.3)$$

Differential equation:

$$\frac{\mathrm{d}Q_{Al}}{\mathrm{d}t} = P_{Al,PfAl} - U_{Al,AlEx} \quad (1.4)$$

Auxiliary equations:

$$U_{Pf,PfAl} = \left(v^{**}_{Al,PfAl} + \left(v^{*}_{Al,PfAl} - v^{**}_{Al,Pf}\right) / \left(1 + (M_{Al,PfAl} / \mathrm{MEIM})^{\theta_{Al,PfAl}}\right)\right) \mathrm{BW} \quad (1.5)$$

$$Y_{Al,PpAl} = v^{**}_{Al,PpAl} + \left(v^{*}_{Al,PpAl} - v^{**}_{Al,PpAl}\right) / (1 + \left(\mathrm{Sl}_{\mathrm{Flow}} / M_{Al,PpAl}\right)^{\theta_{Al,PpAl}}) \quad (1.6)$$

$$v_{pH,SlOl} = \exp\left(-\theta_{Sl,SlOl}\left(pH_{Lu} - v^{(o)}_{pH,SlOl}\right)^2\right) \quad (2.5)$$

Starch in the Lumen, Q_{Sl} mol

Concentration:

$$C_{Sl} = Q_{Sl} / V_{Lu} \quad (2.1)$$

Input:

$$D_{Sl} = \text{driving variable} \quad (2.2)$$

Outputs:

$$U_{Sl,SlEx} = k_p Q_{Sl} \quad (2.3)$$

$$U_{Sl,SlOl} = \left(v_{Sl,SlOl} v_{pH,SlOl} Q_{Al}\right) / \left(1 + \left(M_{Sl,SlOl}\left(T_{Sl} / T_{Sl}^{*}\right)\right) / \left(C_{Sl}\right)\right) \quad (2.4)$$

Auxiliary equation:

$$v_{pH,SlOl} = \exp\left(-\theta_{Sl,SlOl}\left(pH_{Lu} - v_{pH,SlOl}^{(o)}\right)^2\right) \quad (2.5)$$

Differential equation:

$$\frac{\mathrm{d}Q_{Sl}}{\mathrm{d}t} = D_{Sl} - U_{Sl,SlEx} - U_{Sl,SlOl} \quad (2.6)$$

Glucose in Lumen, Q_{Gl} mol

Concentration:

$$C_{Gl} = Q_{Gl} / V_{Lu} \quad (3.1)$$

Inputs:

$$D_{Gl} = \text{ driving variable} \quad (3.2)$$

$$P_{Gl,GuGl} = U_{Gu,GuGl} \quad (3.3)$$

Outputs:

$$U_{Gl,GlGu} = k_{Gl,GlGu}^{(d)} S_{Lu} C_{Gl} \quad (3.4)$$

$$U_{Gl,GlEx} = k_p Q_{Gl} \quad (3.5)$$

Differential equation:

$$\frac{\mathrm{d}Q_{Gl}}{\mathrm{d}t} = D_{Gl} + P_{Gl,GuGl} - U_{Gl,GlGu} - U_{Gl,GlEx} \quad (3.6)$$

Oligosaccharide in Lumen, Q_{Ol} mol

Concentration:

$$C_{Ol} = Q_{Ol} / V_{Lu} \quad (4.1)$$

Inputs:

$$D_{Ol} = \text{ driving variable} \quad (4.2)$$

$$P_{Ol,SlOl} = U_{Sl,SlOl} \quad (4.3)$$

$$P_{Ol,OuOl} = U_{Ou,OuOl} \quad (4.4)$$

Outputs:

$$U_{Ol,OlOu} = S_{Lu} k^{(d)}_{Ol,OlOu} C_{Ol} \quad (4.5)$$

$$U_{Ol,OlEx} = k_p Q_{Ol} \quad (4.6)$$

Differential equation:

$$\frac{\mathrm{d}Q_{Ol}}{\mathrm{d}t} = D_{Ol} + P_{Ol,SlOl} + P_{Ol,OuOl} - U_{Ol,OlOu} - U_{Ol,OlEx} \quad (4.7)$$

Duodenal Unstirred Water Layer (UWL)

Glucose in UWL, Q_{Gu} mol

Concentration:

$$C_{Gu} = Q_{Gu} / V_{Wl} \quad (5.1)$$

Inputs:

$$P_{Gu,GlGu} = U_{Gl,GlGu} \quad (5.2)$$

$$P_{Gu,OuGu} = Y_{Gu,OuGu} U_{Ou,OuGu} \quad (5.3)$$

$$P_{Gu,GbGu} = U_{Gb,GbGu} \quad (5.4)$$

Outputs:

$$U_{Gu,GuGl} = S_{Lu} k^{(d)}_{Gu,GuGl} C_{Gu} \quad (5.5)$$

$$U_{Gu,GuGb} = S_{Lu} k^{(d)}_{Gu,GuGb} C_{Gu} \quad (5.6)$$

$$U_{Gu,GuGe} = \left(v_{Gu,GuGe} S_{Lu}\right) / \left(1 + M_{Gu,GuGe} / C_{Gu}\right) \quad (5.7)$$

Differential equation:

$$\frac{\mathrm{d}Q_{Gu}}{\mathrm{d}t} = P_{Gu,GlGu} + P_{Gu,OuGu} + P_{Gu,GbGu} - U_{Gu,GuGl} - U_{Gu,GuGb} - U_{Gu,GuGe} \quad (5.8)$$

Auxillary equations:

$$v_{Gu,GuGe} = v^{**}_{Gu,GuGe} + \left(\left(v^{*}_{Gu,GuGe} - v^{**}_{Gu,GuGe} \right) / \left(1 + \left(M_{\mathrm{NSC},GuGe} / \mathrm{NSC}_{\mathrm{Flow}} \right)^{\theta_{Gu,GuGe}} \right) \right) \quad (5.9)$$

$$\mathrm{NSC}_{\mathrm{Flow}} = k_p \left(Q_{Gl} + Q_{Ol} + Q_{Sl} \right) \quad (5.10)$$

$$\mathrm{Sl}_{\mathrm{Flow}} = k_p Q_{Sl} \quad (5.11)$$

Oligosaccharide in UWL, Q_{Ou} mol

Concentration:

$$C_{Ou} = Q_{Ou} / V_{Wl} \quad (6.1)$$

Input:

$$P_{Ou,OlOu} = U_{Ol,OlOu} \quad (6.2)$$

Outputs:

$$U_{Ou,OuGu} = \left(v_{Ou,GuDu} S_{Lu} \right) / \left(1 + M_{Ou,OuGu} / C_{Ou} \right) \quad (6.3)$$

$$U_{Ou,OuOl} = S_{Lu} k^{(d)}_{Ou,OuOl} C_{Ou} \quad (6.4)$$

Differential equation:

$$\frac{\mathrm{d}Q_{Ou}}{\mathrm{d}t} = P_{Ou,OlOu} - U_{Ou,OuGu} - U_{Ou,OuOl} \quad (6.5)$$

Auxiliary equations:

$$v_{Ou,GuDu} = v^{*}_{Ou,OuGu} Q_{Oc} v_{pH,OuGu} \quad (6.6)$$

$$v_{pH,OuGu} = \exp\left(-\theta_{Ou,OuGu} \left(pH_{Wl} - v^{(o)}_{pH,OuGu} \right)^2 \right) \quad (6.7)$$

Duodenal Enterocyte

Glucose in enterocyte, Q_{Ge} mol

Concentration:

$$C_{Ge} = Q_{Ge} / V_{En} \quad (7.1)$$

Inputs:

$$P_{Ge,GuGe} = U_{Gu,GuGe} \quad (7.2)$$

$$P_{Ge,GbGe} = U_{Gb,GbGe} \quad (7.3)$$

Outputs:

$$U_{Ge,GeGb} = [\left(v^{**}_{Ge,GeGb} S_{Lu}\right) + \left(\left(v^{*}_{Ge,GeGb} - v^{**}_{Ge,GeGb}\right) S_{Lu}\right) / \left(1 + \left(M_{\mathrm{NSC},GeGb} / \mathrm{NSC}_{\mathrm{Flow}}\right)^{\theta_{Ge,GeGb}}\right)] / \left(1 + M_{Ge,GeGb} / C_{Ge}\right) \quad (7.4)$$

$$U_{Ge,GeOx} = R_{Ge,GuGe} U_{Gu,GuGe} + R_{Gu,AuAe} U_{Au,AuAe} + 0.0043 S_{Lu} \quad (7.5)$$

Differential equation:

$$\frac{\mathrm{d}Q_{Ge}}{\mathrm{d}t} = P_{Ge,GuGe} + P_{Ge,GbGe} - U_{Ge,GeGb} - U_{Ge,GeOx} \quad (7.6)$$

Blood

Blood Glucose, Q_{Gb} mol

$$U_{Gb,GbGu} = k^{(d)}_{Gb,GbGu} C_{Gb} S_{Lu} \quad (8.1)$$

$$U_{Gb,GbGe} = [\left(v^{**}_{Ge,GeGb} S_{Lu}\right) + \left(\left(v^{*}_{Ge,GeGb} - v^{**}_{Ge,GeGb}\right) S_{Lu}\right) / \left(1 + \left(M_{\mathrm{NSC},GeGb} / \mathrm{NSC}_{\mathrm{Flow}}\right)^{\theta_{Ge,GeGb}}\right)] / \left(1 + M_{Gb,GbGe} / C_{Gb}\right) \quad (8.2)$$

---

* Displayed is model code representing one small intestinal sub-section, the first proximal duodenum. The model is repeated for each subsection hereafter until the terminal ileum is reached.

Table A1. Definition of symbols for entities and processes represented in the model

Symbol	Entity
Ae	Amino acids in enterocyte
Al	Amylase in lumen
Au	Amino acids in UWL
BW	Liveweight
Du	Duodenum
Ex	Exit to next subsection
Gb	Glucose in blood
Ge	Glucose in enterocyte
Gl	Glucose in lumen
Gu	Glucose in UWL
Il	Ileum
Je	Jejunum
Lu	Lumen
MEIM	Metabolisable energy intake (MEI) to MEI at maintenance ratio
NSC	Non-structural carbohydrate
Oc	Oligosaccharidase
Ol	Oligosaccharide in lumen
Ou	Oligosaccharide in UWL
Pf	Pancreatic fluid
Pp	Pancreatic protein

Sl	Starch in lumen
Wl	Water layer (unstirred)

1169

Table A2. General notation used in the model

Symbol	Entity
C_i	Concentration of *i*, mol/L
D_i	Entry of *i* from passage or infusion (driving variable), mol/h
$k_{i.jk}^{(d)}$	Diffusion constant for *i* in *j* - *k* transaction, /h
k_p	Fractional rate of passage constant, /h
$M_{i,jk}$	Michaelis-Menten affinity constant with respect to *i* for *j* - *k* transaction, mol/L
$P_{i,jk}$	Rate of production of *i* in *j* - *k* transaction, mol/h
pH_i	pH of region *i*
Q_i	Quantity of *i*, mol
$R_{i,jk}$	Requirement for *i* in *j* - *k* transaction, mol/mol
S_i	Surface area of *i*, cm^2
T_i	Digestion turnover time of substrate *i*, h
T_i^*	Maximum level with respect to *i*, h
$\theta_{i,jk}$	Steepness parameter associated with *i* for *j* - *k* transaction
$U_{i,jk}$	Rate of utilization of *i* by *j* - *k* transaction, mol /h
V_i	Effective volume of *i*, L or kg
$v_{i,jk}$	Velocity for *j* - *k* transaction with respect to *i*, mol/h
$v_{i,jk}^*$	Maximum level with respect to *i* for *j* - *k* transaction, mol/h
$v_{i,jk}^{**}$	Minimum level with respect to *i* for *j* - *k* transaction, mol/h

$v_{i,jk}^{(o)}$	Optimum level of *i* for *j* - *k* transaction
$Y_{i,jk}$	Yield of *i* in *j* - *k* transaction, mol/mol

1170